TURUN YLIOPISTO
UNIVERSITY OF TURKU

ANALYTICAL TECHNIQUES FOR X-RAY POLARIZATION STUDIES OF RAPIDLY ROTATING NEUTRON STARS AND BLACK HOLES

Vladislav Loktev

TURUN YLIOPISTON JULKAISUJA ANNALES UNIVERSITATIS TURKUENSIS
SARJA SER. AI OSA TOM. 733 | ASTRONOMICA CHEMICA PHYSICA MATHEMATICA | TURKU 2025

TURUN
YLIOPISTO
UNIVERSITY
OF TURKU

ANALYTICAL TECHNIQUES FOR X-RAY POLARIZATION STUDIES OF RAPIDLY ROTATING NEUTRON STARS AND BLACK HOLES

Vladislav Loktev

TURUN YLIOPISTON JULKAISUJA   ANNALES UNIVERSITATIS TURKUENSIS
SARJA   SER. AI OSA   TOM. 733 | ASTRONOMICA   CHEMICA   PHYSICA   MATHEMATICA | TURKU 2025

University of Turku

Faculty of Science
Department of Physics and Astronomy
Astronomy
Doctoral programme in Exact Sciences

Supervised by

Docent Alexandra Veledina
Department of Physics and Astronomy
University of Turku
Turku, Finland

Professor Juri Poutanen
Department of Physics and Astronomy
University of Turku
Turku, Finland

Reviewed by

Professor M. Coleman Miller
Department of Astronomy
University of Maryland
College Park, MD, USA

Professor Maxim Lyutikov
Department of Physics and Astronomy
Purdue University
West Lafayette, IN, USA

Opponent

Doctor Benoît Cerutti
Institut de Planétologie et d'Astrophysique de Grenoble
Université Grenoble Alpes
Grenoble, France

ISBN 978-952-02-0118-0 (PRINT)
ISBN 978-952-02-0119-7 (PDF)
ISSN 0082-7002 (PRINT)
ISSN 2343-3175 (ONLINE)
Painosalama Oy, Turku, Finland, 2025

UNIVERSITY OF TURKU
Faculty of Science
Department of Physics and Astronomy
Astronomy
LOKTEV, VLADISLAV: Analytical Techniques for X-ray Polarization Studies of Rapidly Rotating Neutron Stars and Black Holes
Doctoral dissertation, 118 pp.
Doctoral programme in Exact Sciences
April 2025

ABSTRACT

Compact stellar remnants such as neutron stars and black holes attract not only material from their surroundings but also the close attention of astronomers. The latter is because these objects constitute unattainable cosmic laboratories that showcase extreme physics on a grand scale. The environments around these objects feature high, near-critical magnetic fields, gravitational warping of spacetime, and highly relativistic motion of matter. In close binary systems, a compact object strips matter from a companion star, forming an accretion disk around itself. Influenced by the intense gravity, matter falling onto a compact object will heat up to very high temperatures and emit X-rays.

X-ray polarimetry emerges as a powerful tool for probing these exceptional systems. Polarization of light is inherently geometric in nature and often carries information about the physical properties of the system that is not accessible through just the intensity of the radiation. Hence, polarization measurements can reveal the structure of magnetic fields, the orientation of accretion disks, and the properties of coronae around them. My work was significantly shaped by the launch of the first X-ray polarimeter in the 21st century, the *Imaging X-ray Polarimetry Explorer (IXPE)* mission. I studied the ways in which we can extract information about the geometry and physical processes in X-ray binary systems from the spectral and polarimetric properties of these X-rays. Two subclasses of X-ray binaries underwent my scrutiny: accreting millisecond pulsars and black hole X-ray binaries.

Accreting millisecond pulsars are neutron stars that accrete matter from a companion star. Over the course of the evolution of the system, the neutron star is spun up to periods of a few milliseconds, and this rotation is so steady that it renders the systems into the most precise clocks in the universe. X-ray radiation emerges near the magnetic poles of the neutron star, and if the magnetic and rotation axes are misaligned, as often happens, the radiation will be pulsed. A longstanding question for neutron stars is the equation of state of the matter in their cores, which connects the mass and radius of the star. Precise measurements and analysis of X-ray pulse profiles can infer the geometrical properties of the system, which in turn can be used to constrain the equation of state of a neutron star. One particular challenge I focused on in my work is posed by the relativistic velocities of the surface of the neutron star, which deforms the neutron star into an oblate shape, affecting the observed pulse profiles.

The black hole X-ray binaries, on the other hand, pose different questions. The

event horizon instead of a solid surface makes it notoriously difficult to infer the spin rate of the black hole. The spin parameter must be inferred from the geometrical properties of the disk of accreting matter that forms around it. In the so-called soft state, the disk is geometrically thin and extends down to the innermost stable circular orbit, which is uniquely characterized by the spin of the black hole. However, constraining the geometry from X-ray spectral properties is not a straightforward task, especially so due to the radiation is twisted by the strong gravity of the black hole. My interest in these systems was to study the ways to connect the spectropolarimetric properties of the X-ray radiation to the geometry of the system in a more quick and flexible way than traditional ray tracing techniques would allow.

TURUN YLIOPISTO
Matemaattis-luonnontieteellinen tiedekunta
Fysiikan ja tähtitieteen laitos
Tähtitiede
LOKTEV, VLADISLAV: Analytical Techniques for X-ray Polarization Studies of Rapidly Rotating Neutron Stars and Black Holes
Väitöskirja, 118 s.
Eksaktien tieteiden tohtoriohjelma
Huhtikuu 2025

TIIVISTELMÄ

Kompaktit tähdet, kuten neutronitähdet ja mustat aukot, vetävät puoleensa sekä ympäröivää ainetta, että tähtitieteilijöiden herkeämätöntä huomiota. Läheisissä kaksoistähtijärjestelmissä tiivis kappale imee ainetta kumppaniltaan muodostaen kertymäkiekon ympärilleen. Voimakkaan painovoiman vaikutuksesta tiiviille kappaleelle putoava aine kuumenee äärimmäisen korkeisiin lämpötiloihin ja säteilee röntgensäteitä.

Röntgensäteiden polarisaation mittaus on osoittautunut tehokkaaksi työkaluksi näiden poikkeuksellisten järjestelmien tutkimisessa. Valon polarisaatio on luonteeltaan geometrista ja sisältää usein tietoa järjestelmän fysikaalisista ominaisuuksista, jota ei voida havaita pelkästään säteilyn voimakkuutta mittaamalla. Täten polarisaatiomittaukset voivat paljastaa magneettikenttien rakenteen, kertymäkiekkojen suuntautumisen ja niitä ympäröivien kuumien kaasukehien eli koronoiden ominaisuuksia. Tutkimustani edisti merkittävästi 2000-luvun ensimmäisen röntgenpolarimetrin, *Imaging X-ray Polarimetry Explorer (IXPE)* mission, laukaisu. Tutkin keinoja, joilla voimme saada tietoa röntgenkaksoistähtijärjestelmien geometriasta ja fysikaalisista prosesseista näiden röntgensäteiden spektri- ja polarisaatio-ominaisuuksien avulla. Tarkasteluni kohteena oli kaksi röntgenkaksoistähtien alaluokkaa: kertyvät millisekuntipulsarit ja mustien aukkojen röntgenkaksoistähdet.

Kertyvät millisekuntipulsarit ovat neutronitähtiä, jotka keräävät ainetta kumppaniltaan. Järjestelmän kehittyessä neutronitähden pyöriminen kiihtyy muutaman millisekunnin jaksoihin, ja tämä pyöriminen on niin vakaata, että nämä järjestelmät toimivat maailmankaikkeuden tarkimpina kelloina. Röntgensäteily syntyy neutronitähden magneettisten napojen lähellä, ja jos magneettiset ja pyörimisakselit ovat erisuuntaiset, mikä on yleistä, säteily on pulssimaista. Keskeinen kysymys neutronitähdissä koskee niiden ytimien aineen tilanyhtälöä, joka kytkee tähden massan ja säteen toisiinsa. Röntgenpulssiprofiilien tarkat mittaukset ja analyysit voivat paljastaa järjestelmän geometriset ominaisuudet, joita voidaan puolestaan käyttää neutronitähden tilanyhtälön rajoittamiseen. Yksi erityinen haaste, johon keskityin työssäni, on neutronitähden pinnan suurten nopeuksien aiheuttama litistyminen, joka vaikuttaa havaittuihin pulssiprofiileihin.

Mustien aukkojen röntgenkaksoistähdet puolestaan herättävät erilaisia kysymyksiä. Kiinteän pinnan puuttuminen ja tapahtumahorisontin olemassaolo tekee mustan aukon pyörimisnopeuden määrittämisestä erityisen vaikeaa. Pyörimisnopeus on

pääteltävä mustan aukon ympärille muodostuvan kertymäkiekon geometrisista ominaisuuksista. Niin kutsutussa pehmeässä tilassa kiekko on geometrisesti ohut ja ulottuu sisimpään vakaaseen ympyrärataan asti, jonka sijainti määräytyy yksiselitteisesti mustan aukon pyörimisnopeudesta. Geometrian määrittäminen röntgenspektrin ominaisuuksista ei kuitenkaan ole suoraviivaista, erityisesti koska mustan aukon voimakas painovoima vääristää säteilyä. Kiinnostukseni näitä järjestelmiä kohtaan keskittyi tapoihin yhdistää röntgensäteilyn spektri- ja polarisaatio-ominaisuudet järjestelmän geometriaan nopeammin ja joustavammin kuin perinteiset säteenseurantatekniikat mahdollistavat.

Acknowledgements

It is often said that a PhD thesis is a reflection of one's journey, both academic and personal. I am filled with gratitude towards the individuals who have supported, guided, and inspired me along the way.

First and foremost, I would like to express my deepest appreciation to Professor Juri Poutanen, the leader of our high-energy astrophysics group and my supervisor. Their unreserved support, thoughtful insights, and patience played a crucial role in the completion of this thesis. His unparalleled expertise as well as his mental and executive capacity have been a huge inspiration to me and have contributed invaluably to my academic growth. I would like to express my sincere gratitude to docent Alexandra Veledina, who has been my primary mentor, for pushing me beyond my comfort zone and for challenging me to think critically. Without the complementary expertise and encouragement of my supervisors, this thesis would not have been possible. I am forever grateful for the countless hours they have invested in nurturing my academic development and truly honored to have had the opportunity to learn from them.

I am also indebted to my collaborators, Joonas Nättilä, Tuomo Salmi, Valery Suleimanov, and Anna Bobrikova, whose ideas and tireless efforts have contributed to the success of my research. Their willingness share their knowledge and put in the hard work have been invaluable. I am thankful to Valery Suleimanov for the hospitality during my visits to the Tübingen University. I am specially grateful to Joonas Nättilä and Vladimir Zhdankin for their guidance and helpful support during my research stays at the Center for Computational Astrophysics in Flatiron Institute. This experience has significantly broadened my research perspectives and has been a highlight of my doctoral journey.

Moreover, I would like to thank Professor M. Coleman Miller and Professor Maxim Lyutikov for rigorous pre-examination of this thesis and valuable insights that have helped me improve this work. I thank Doctor Benoît Cerutti for agreeing to become my esteemed opponent.

My heartfelt thanks also go out to the current and past members of the high-energy astrophysics group. As my journey unfolded for a long time, the list of people who have been part of the group is also long. My sincere gratitude goes to Pavel Abolmasov, Anna Chashkina, Tuomo Salmi, Juhani Mönkkönen, Vadim Kravtsov, Anna Bobrikova, Armin Nabizadeh, Ilia Kosenkov, Sofia Forsblom, Anagha Nitindala, Varpu Ahlberg, Yannis Liodakis, and María Alejandra Díaz. Coffee breaks, lunchtime discussions, and occasional group trips during conferences and workshops have provided a friendly and pleasant environment that I am grateful to have been a part of.

Importantly, I would like to acknowledge the financial support provided by the Jenny and Antti Wihuri Foundation, Vilho, Yrjö and Kalle Väisälä Fund, and the University of Turku. Their generous stipends and grants have allowed me to focus on my studies without the added burden of financial stress. I would like to extend my gratitude to the faculty and staff of the University of Turku, who have provided me with a supportive academic environment and the necessary resources to undertake this research. I would also like to acknowledge the Saint Petersburg State University, the alma mater of both my supervisors and myself, for enabling and facilitating the start of our collaboration outside of it.

Finally, I wish to express my gratitude to my family, especially my father and uncle whose support, despite the distance separating us across the border, made this journey possible. The thought that my mother would have been proud of this achievement has also been a source of strength during difficult times.

March 2025
Vladislav Loktev

Table of Contents

Abbreviations

AGN	Active Galactic Nuclei
AMP	accreting millisecond pulsar
BH	black hole
EM	electro-magnetic
EoS	equation of state
eXTP	Enhanced X-ray Timing and Polarimetry mission
GR	general relativity
HID	hardness-intensity diagram
HMXB	high-mass X-ray binary
ISCO	innermost stable circular orbit
IXPE	Imaging X-ray Polarimetry Explorer
LMXB	low-mass X-ray binary
NASA	National Aeronautics and Space Agency
NS	neutron star
PA	polarization angle
PD	polarization degree
SR	special relativity
SSC	synchrotron self-Compton
ULX	Ultraluminous X-ray source
XRB	X-ray binary

List of Original Publications

The original publication listed below form the basis of this dissertation and are cited throughout using respective Roman numerals.

I Loktev V., Salmi T., Nättilä J., Poutanen J.
Oblate Schwarzschild approximation for polarized radiation from rapidly rotating neutron stars.
Astronomy & Astrophysics, 2020; 643: A84.

II Salmi T., Loktev V., Korsman K., Baldini L., Tsygankov S. S., Poutanen J.
Neutron star parameter constraints for accretion-powered millisecond pulsars from the simulated IXPE data.
Astronomy & Astrophysics, 2021; 646: A23.

III Bobrikova A., Loktev V., Salmi T., Poutanen J.
Polarized radiation from an accretion shock in accreting millisecond pulsars using exact Compton scattering formalism.
Astronomy & Astrophysics, 2023; 678: A99.

IV Loktev V., Veledina A., Poutanen J.
Analytical techniques for polarimetric imaging of accretion flows in the Schwarzschild metric.
Astronomy & Astrophysics, 2022; 660: A25.

V Loktev V., Veledina A., Poutanen J., Nättilä J., Suleimanov V. F.
ARTPOL: Analytical ray-tracing method for spectro-polarimetric properties of accretion disks around Kerr black holes.
Astronomy & Astrophysics, 2024; 685: A84.

List of publications not included in the thesis

VI Krawczynski H., Muleri F., Dovčiak M., Veledina A., Rodriguez Cavero N., Svoboda J., Ingram A., Matt G., Garcia J. A., Loktev V., et al.
Polarized x-rays constrain the disk-jet geometry in the black hole x-ray binary Cygnus X-1.
Science, 2022; 378: 650.

VII Illiano G., Papitto A., Sanna A., Bult P., Ambrosino F., Miraval Zanon A., Coti Zelati F., Stella L., Altamirano D., Baglio M. C., Bozzo E., Burderi L., de Martino D., Di Marco A., di Salvo T., Ferrigno C., Loktev V., Marino A., Ng M., Pilia M., Poutanen J., Salmi T.
Timing Analysis of the 2022 Outburst of the Accreting Millisecond X-Ray Pulsar SAX J1808.4-3658: Hints of an Orbital Shrinking.
The Astrophysical Journal, 2023; 942: L40.

VIII Doroshenko V., Poutanen J., Heyl J., Tsygankov S. S., Caiazzo I., Turolla R., Veledina A., Weisskopf M. C., Forsblom S. V., González-Caniulef D., Loktev V., et al.
Complex variations in X-ray polarization in the X-ray pulsar LS V +44 17/RX J0440.9+4431.
Astronomy and Astrophysics, 2023; 677: A57.

IX Ingram A., Ewing M., Marinucci A., Tagliacozzo D., Rosario D. J., Veledina A., Kim D. E., Marin F., Bianchi S., Poutanen J., Matt G., Marshall H. L., Ursini F., De Rosa A., Petrucci P.-O., Madejski G., Barnouin T., Gesu L. D., Dovčiak M., Gianolli V. E., Krawczynski H., Loktev V., et al.
The X-ray polarization of the Seyfert 1 galaxy IC 4329A.
Monthly Notices of the Royal Astronomical Society, 2023; 525: 5437.

X Ratheesh A., Dovčiak M., Krawczynski H., Podgorný J., Marra L., Veledina A., Suleimanov V. F., Rodriguez Cavero N., Steiner J. F., Svoboda J., Marinucci A., Bianchi S., Negro M., Matt G., Tombesi F., Poutanen J., Ingram A., Taverna R., West A., Karas V., Ursini F., Soffitta P., Capitanio F., Viscolo D., Manfreda A., Muleri F., Parra M., Beheshtipour B., Chun S., Cibrario N., Di Lalla N., Fabiani S., Hu K., Kaaret P., Loktev V., et al.
X-Ray Polarization of the Black Hole X-Ray Binary 4U 1630–47 Challenges the Standard Thin Accretion Disk Scenario.
The Astrophysical Journal, 2024; 964: 77.

XI Ingram A., Bollemeijer N., Veledina A., Dovčiak M., Poutanen J., Egron E., Russell T. D., Trushkin S. A., Negro M., Ratheesh A., Capitanio F., Connors R., Neilsen J., Kraus A., Iacolina M. N., Pellizzoni A., Pilia M.,

Carotenuto F., Matt G., Mastroserio G., Kaaret P., Bianchi S., García J. A., Bachetti M., Wu K., Costa E., Ewing M., Kravtsov V., Krawczynski H., Loktev V., et al.
Tracking the X-Ray Polarization of the Black Hole Transient Swift J1727.8–1613 during a State Transition.
The Astrophysical Journal, 2024; 968: 76.

XII Steiner J. F., et al.
An IXPE-led X-Ray Spectropolarimetric Campaign on the Soft State of Cygnus X-1: X-Ray Polarimetric Evidence for Strong Gravitational Lensing.
The Astrophysical Journal, 2024; 969: L30.

XIII Bobrikova A., Forsblom S. V., Di Marco A., La Monaca F., Poutanen J., Ng M., Ravi S., Loktev V., et al.
Discovery of a strong rotation of the X-ray polarization angle in the galactic burster GX 13+1.
Astronomy and Astrophysics, 2024; 688: A170.

XIV Bobrikova A., Di Marco A., La Monaca F., Poutanen J., Forsblom S. V., Loktev V.
New polarimetric study of the galactic X-ray burster GX 13+1.
Astronomy and Astrophysics, 2024; 688: A217.

XV Veledina A., Poutanen J., Bocharova A., Di Marco A., Forsblom S. V., La Monaca F., Podgorný J., Tsygankov S. S., Zdziarski A. A., Ahlberg V., Green D. A., Muleri F., Rhodes L., Bianchi S., Costa E., Dovčiak M., Loktev V., McCollough M., Soffitta P., Sunyaev R.
Ultrasoft state of microquasar Cygnus X-3: X-ray polarimetry reveals the geometry of the astronomical puzzle.
Astronomy and Astrophysics, 2024; 688: L27.

XVI Veledina A., Muleri F., Poutanen J., Podgorný J., Dovčiak M., Capitanio F., Churazov E., De Rosa A., Di Marco A., Forsblom S. V., Kaaret P., Krawczynski H., La Monaca F., Loktev V., et al.
Cygnus X-3 revealed as a Galactic ultraluminous X-ray source by IXPE.
Nature Astronomy, 2024; 8: 1031.

1 X-ray binaries

All black holes are alike; each neutron star is neutron in its own way.

Approximately one-third of all stars in our Galaxy are part of a binary system, according to various estimates and surveys (Lada 2006; De Rosa et al. 2014). This proportion is even higher among massive stars (Preibisch et al. 2001; Grellmann et al. 2015). When a massive star reaches the end of its life cycle, it typically explodes in a supernova, leaving behind a compact object like a neutron star (NS) or a black hole (BH). The presence of a companion star adds layers of complexity, leading to various peculiar co-evolutionary stages.

The companion star can lose matter through mechanisms such as Roche Lobe overflow or strong stellar winds. This lost matter is then captured by the compact object's gravitational well, forming an accretion disk around it. However, the accretion process is far from simple. In different cases and different states, the system can include additional components like jets, accretion columns, winds, and hot coronae. Importantly, these components do not just co-exist; they interact in complex ways, influenced by the curvature of spacetime around the compact object, extreme magnetic fields, intense X-ray radiation, and other high-energy astrophysical phenomena. The process also exhibits vast timing phenomenology such as changes of state, pulsations, and quasi-periodic oscillations.

This complex arrangement is what defines an X-ray binary (XRB). In its essence, an XRB is an extraordinary laboratory in outer space that serves as an interface between numerous extreme physical processes. They encompass a large portion of diverse problems in high energy astrophysics (Longair 2011) ever since their discovery in 1962 (Giacconi et al. 1962).

1.1 Different compact objects

The reasons why some scientists focus on BHs while others study NSs can vary. BHs are the ultimate embodiment of gravity. Their properties challenge the theories of fundamental physics, such as the clash between general relativity and quantum mechanics. On the other hand, NSs naturally host a laboratory for studying the properties of matter under immense densities and pressures and testing the theories of nuclear physics, the strong nuclear force. As fascinating as BH phenomena may be, the BHs are simple, with only mass and spin completely describing them. For instance, the radius of a BH scales proportionally to the mass. The relation between the size and mass of the NS, in turn, is infamously unknown and often remains the main focus of astrophysical investigations. On the other hand, when a NS exhibits pulsations, its spin period can be very precisely measured, to the point that some millisecond pulsars can compete with the most precise atomic clocks on Earth. But now the spin of a BH, that is the amount of its angular momentum, in turn, is impossible to measure directly, as BHs have no surface, and the existing methods to infer the spin often produce discrepancies in spin estimates. Ultimately, both BHs and NSs represent unique challenges and opportunities to push the boundaries of fundamental physics, (for a more in-depth review, see Miller & Miller 2015).

1.1.1 Neutron stars, accretion columns

Once a star fuses all the nuclei of light elements into heavier ones up to iron, the pressure generated by the thermonuclear synthesis can no longer balance the gravity, and the core must collapse. If the progenitor star is not heavy enough, then, in the final stage the electron degeneracy pressure in the core is going to be strong enough to match the gravity, and the core will become a white dwarf instead of a NS. On the other hand, if the core is too massive, at a certain point the neutron degeneracy pressure and the strong nuclear forces will not be enough to match the gravity, and the star collapses into a BH. Thus, there are some limits on the possible mass of the NS. The Chandrasekhar limit of about 1.4 solar masses (Chandrasekhar 1931) is the maximum mass for a white dwarf to exist and as the iron cores of the massive stars that collapse into NSs are somewhat degenerate, the typical mass of a NS born from a core-collapse supernovae is about 1.3-1.4 solar masses (Timmes et al. 1996). The lightest stars that produce a NS as their remnant, can form NSs of about 1.2 solar masses. However, much lighter NSs are sometimes claimed (Doroshenko et al. 2022b); if such neutron stars exist, they might form via an exotic path. On the other hand, the Tolman–Oppenheimer–Volkoff limit of between 2.2 and 2.9 solar masses (Kalogera & Baym 1996), is the theoretical maximum. From an observational perspective, the highest precise and reliable measurement of a NS mass among Galactic pulsars is about 2.1 solar masses (Fonseca et al. 2021, for PSR J0740+6620). Claims of higher NSs mass, up to about 2.6 solar masses, exist for ms-pulsars (Freire et al. 2008), X-ray pulsars (Clark et al. 2002), and gravitational wave sources (Abbott et al. 2020).

In turn, the theoretical limits on the size of a NS depend on the equation of state (EoS) in its core and the crust. The radii of NSs are measured to be between 10 and 15 km (Lattimer & Prakash 2004; Özel & Freire 2016). A mass of a typical stellar core confined in such a small volume makes the central densities exceed nuclear density $\approx 2.8 \times 10^{14}$ g cm^{-3}. The EoS of the matter this dense is one of the biggest questions on the interface between nuclear physics and high-energy astrophysics, and one of the main reasons to study NSs in the first place. The EoS is directly constrained by both the radius and the mass of the stellar remnant through Tolman-Oppenheimer-Volkoff equations (Tolman 1939; Oppenheimer & Volkoff 1939). As there is no way to measure these parameters of the objects directly, the best way to obtain them is to study the various phenomena that NSs exhibit, understand the physics of the processes, and infer the parameters of the object that could have possibly produced the phenomena in question. So far, even the most accurate methods of mass and radius measurement (Nättilä et al. 2016; Raaijmakers et al. 2021) still leave many EoSs consistent with the measurement. More methods to tighten the constraints on NSs are always welcome. X-ray polarization measurements of XRBs with NSs is one of the newest available such methods (Poutanen 2020) capable of constraining the geometrical parameters of accretion.

In an accreting NS binary system, the material for accretion is typically provided by a companion star. Depending on the nature of the companion and the binary separation, the accretion can proceed through a few different channels. In the case of a high magnetic field (and it may reach $\sim 10^{12}$ G and higher), the highly ionized accreting plasma encounters the strong magnetic field of a NS at the magnetospheric radius R_{m}. The magnetic pressure is too high for the plasma to flow inwards across the field lines. The flow then funnels along the field lines and continues falling onto the magnetic poles, forming hotspots on the NS surface or accretion columns that can reach tens of kilometers above the surface, depending on the accretion rate (a recent review on the topic Mushtukov & Tsygankov 2024). The accreted plasma loses its gravitational energy near the surface, emitting X-rays and sometimes gamma-rays (see the scheme in Fig. 1). For strongly magnetized NSs like typical pulsars, R_{m} is large and the columns tend to have cylindrical structure, while typically more weakly magnetized millisecond pulsars ($B \sim 10^8$ G) have R_{m} much closer to the surface, leading to funnel flows and hotspots of elongated shape (Romanova et al. 2004). And on the other extreme, some NSs do not possess a high enough magnetic field to channel the accretion flow, so the plasma meets the NS surface at its equator (Syunyaev & Shakura 1986).

Polarization information can give fruitful insights both into strongly magnetized X-ray pulsars (Mushtukov & Tsygankov 2024) and weakly magnetized NSs (Gnarini et al. 2022). Some results for accreting millisecond pulsars are also expected (Bobrikova et al. 2023). So far the polarization information helped to identify the inclinations of several X-ray pulsars (for example Tsygankov et al. 2022; Mushtukov et al. 2023), discover additional components of polarized emission (Doroshenko et al. 2023), detect possible misalignments between NS spin and the binary orbit in a number of different sources, and overall detect the unexpected polarimetric behavior of NS-XRBs and challenge the polarization mechanisms themselves in these objects (Capitanio et al. 2023).

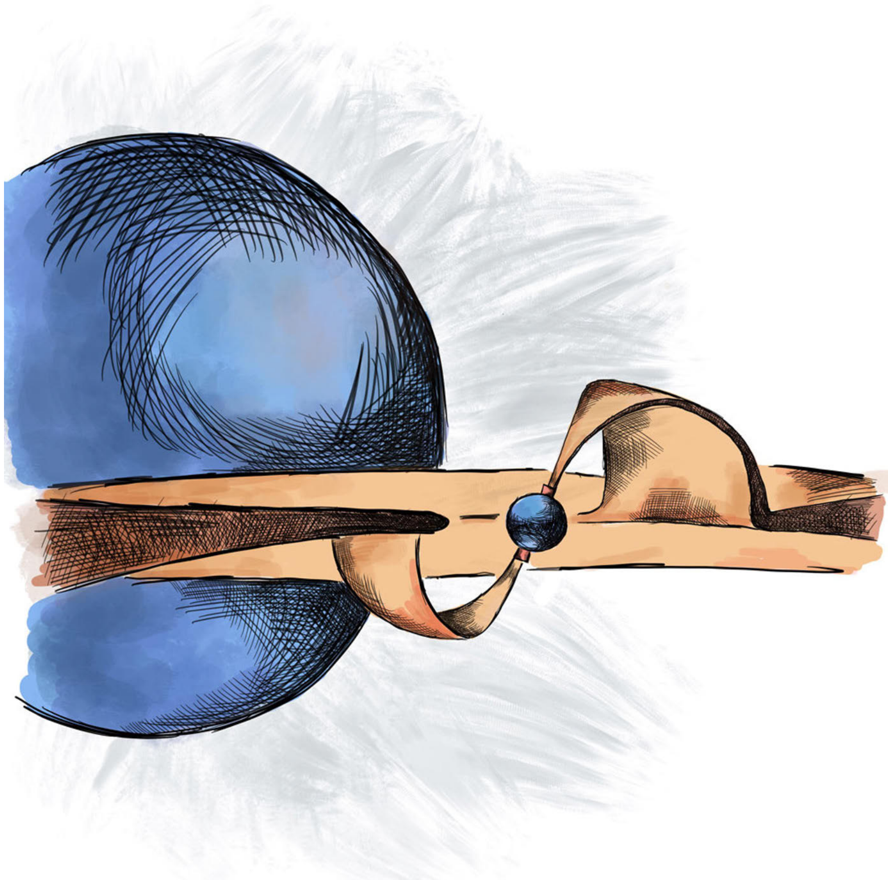

Figure 1. The schematic representation of an accreting NS in an XRB. From Tsygankov et al. (2022).

With a strong magnetic field, the polarization of this radiation will be dominated by the dipole component of the field and will oscillate with the magnetic axis of the pulsar (Mushtukov & Tsygankov 2024). Thus, the it becomes possible to model the orientation of the polarization plane using the rotating vector model (Radhakrishnan & Cooke 1969; Poutanen 2020). The polarization parameters will be mathematically defined and discussed in more detail in chapter 2. In principle, the inclination of the rotation axis and the magnetic dipole axis can be constrained by the precise timing of the polarization direction alone. The intensity of the radiation and the fraction of polarization will depend on the structure of the shock wave at the collision site. Factors such as spot size, cyclotron resonance, temperature structure, shape and height of the accretion column may play a role. Correct accounting of all these factors allows for obtaining accurate pulse and polarization profiles, which in turn allows for constraining the parameters of the NS.

NSs also show other types of characteristic variability, such as glitches in the pulsation period (Zhou et al. 2022; Haskell & Melatos 2015), or thermonuclear bursts in X-ray radiation and oscillations (Watts 2012; Galloway & Keek 2021). Such phenomena can be used to constrain the EoS of matter inside the NS and to estimate the parameters of the EoS. In the articles that are part of this work, we focus on methods for modeling pulse profiles and evaluate the possibilities for constraining NS parameters from X-ray polarization data.

1.1.2 Black holes, accretion disks

Unlike NSs, BHs do not have a solid surface for matter to crash into to generate bright X-ray radiation, and therefore the bulk of high energy emission originates from the accretion flows in the vicinity of the BH. These include the accretion disk, the inner parts of the hot flow, relativistic winds, coronae, and jets (see in Fig. 2). However, the main component is the accretion disk. The matter from the companion star forms a flattened, differentially rotating structure, where friction and turbulence transport angular momentum outwards while the gas slowly spirals inwards. There, orbital shearing heats the gas to extreme temperatures, and gravitational energy converts into intense X-ray emission.

One of the most interesting and key tasks regarding accreting BHs is determining their masses and spins. A number of various methods based on models of observed X-ray spectra are established for this task. One of the main approaches is based on the analysis of the X-ray continuum. This method uses the fact that the inner edge of the accretion disk depends on the spin of the BH: the faster the BH spins in the direction of disk rotation, the closer the inner edge of the disk is to it. Thus, by measuring the temperature of the disk's inner edge, one can estimate the spin.

An additional important component of the observed spectrum of accretion disks is relativistic X-ray reflection. It appears when the high-energy photons from the hot medium above the disk (corona or, in some models, jet) interact with the cooler matter of the disk. As a result, a characteristic reflection spectrum is formed, including a Compton hump at energies around 30 keV and emission lines, the most notable of which is the iron Kα line at 6.4 keV. The iron Kα line is formed in the process of fluorescence, when high-energy photons knock out electrons from the K-shell of iron atoms, followed by the transition of an electron from the L-shell with the emission of a photon. The profile of this line is strongly distorted by relativistic effects near the BH, including gravitational lensing and the Doppler effect (Miniutti & Fabian 2004). Obtaining information about the geometry of the inner regions of the disk and the BH spin is facilitated by modeling these distortions and analyzing the shape of the Fe Kα line. These are, however, also strongly model-dependant on the positioning and nature of the primary source of X-rays (Markoff et al. 2005).

Another method is based on the analysis of time delays (timing) between different energy ranges of X-ray radiation. This approach assumes that the nature of the delays lies in reverberation, the X-ray echo from the different parts of the accretion disk surface. The primary source of X-rays that are reflected from the disk is some hot corona above the disk, the nature of which is not entirely clear. Thus, these data also contain information about the size and geometry of the disk. However, the method can be fruitful for determining some parameters of BHs in XRBs (see e.g. Mastroserio et al. 2018). One broad area of research related to timing that is worth mentioning is the observation and modeling of quasi-periodic oscillations in X-ray radiation, it can also be used to constrain the spin of the BH. This effect could be associated with the precession of the inner parts of the accretion disk (Ingram et al. 2009) superimposed on fluctuations in the accretion rate (Ingram & Done 2011). The results of numerical simulations show that the precession effect can play an important role in the dynamics of accretion flows and affect the orientation of jets (see e.g. Liska et al. 2021), which in turn can have implications for X-ray spectral analysis (for a review see Ingram & Motta 2019) and strongly tied to the spin of the BH.

However, the spin values obtained by different methods often do not agree with each other (Reynolds 2021), indicating the need for further improvement of models and measurement techniques. In particular, observation of X-ray polarization can resolve these contradictions by eliminating models inconsistent with polarization properties and refining the spin taking into account polarization effects in the corresponding methods. In the work comprising this dissertation, we primarily focus on the continuum fitting method with polarization.

The matter in the accretion disks around BHs can exist in various states modeled by its different geometry and physical properties. The standard disk model (Shakura & Sunyaev 1973; Novikov & Thorne 1973), is a geometrically thin, optically thick structure where radiation cooling occurs efficiently. This type of disk is usually observed in the high/soft state of XRBs, where it is stretches all the way down to the innermost stable orbit (Done et al. 2007). In contrast, the advection-dominated accretion flow (ADAF) is a geometrically thick, optically thin disk where cooling is inefficient, and most of the energy is advected into the BH. ADAF is usually associated with the low/hard state (Esin et al. 1997). The magnetically arrested disk (MAD) is a configuration where the magnetic field is so strong that it partially suppresses accretion (Narayan et al. 2003). This model is widely considered for the accretion flows around supermassive BHs and Active Galactic Nuclei (AGN) (Yuan & Narayan 2014). In this case, the structure of the magnetic field in the accretion flow becomes important for the polarization in radio (for example, see Event Horizon Telescope Collaboration et al. 2021). In the work comprising this dissertation, we primarily focus on standard disk models, although the perspective is to explore all the possibilities for different geometries and structures in different states of BH accretion.

In addition to accretion, significant outflows of matter are expected in BH systems, because angular momentum needs to transfer outward to enable accretion. Moreover, the high luminosity of the accretion disk can create radiation pressure sufficient to eject part of the matter in the form of winds. When the BH is seen through the material of such winds, a part of the observed X-ray radiation is reprocessed by scattering in the wind, which modifies the spectral parameters and can introduce an additional source of polarization (Tomaru et al. 2024). Furthermore, relativistic jets are observed directly in the radio range — these are collimated plasma flows ejected, supposedly, along the rotation axis of the BH (Fender et al. 2004) at velocities often close to the speed of light (Mirabel & Rodríguez 1999). In the X-ray range, direct observation of jets is difficult, although at times possible for some XRBs (Heinz et al. 2007) as well as AGN (Feigelson et al. 1981; Marshall et al. 2005). However, there are strong correlations between X-ray and radio emission, indicating a close connection between processes in the accretion disk and jet formation (Merloni et al. 2003; Gallo et al. 2003). Explanations for the mechanisms of jet formation include magnetohydrodynamic processes, such as the Blandford-Znajek mechanism (Blandford & Znajek 1977), where energy is extracted from a rotating BH through magnetic fields, or Blandford-Payne process (Blandford & Payne 1982), where the energy is extracted from the accretion disk itself through the magnetic lines threading through it. However, a detailed understanding of particle acceleration processes in jets and their radiation mechanisms still requires further research.

1.2 Types of X-ray binaries

XRBs come in two types: high-mass X-ray binaries (HMXBs) and low-mass X-ray binaries (LMXBs). This classification is determined by the mass of the donor star, a star serving as the source of material being accreted onto the compact object. The type of the companion star influences accretion structure, spectral behavior, and how XRBs evolve over time.

1.2.1 High mass X-ray binaries

HMXBs have relatively young, massive companion stars. These stars typically belong to the class of supergiants of O or B spectral type (Lutovinov et al. 2013). The massive stars evolve and burn out comparatively quickly due to more extreme condition in their cores and their lifetimes are typically in the range of a few million years. The age of the system as a whole is confined to be within the typical lifetime of massive stars. Reflecting their relatively young age, HMXBs are typically located in star-forming regions in the galactic plane.

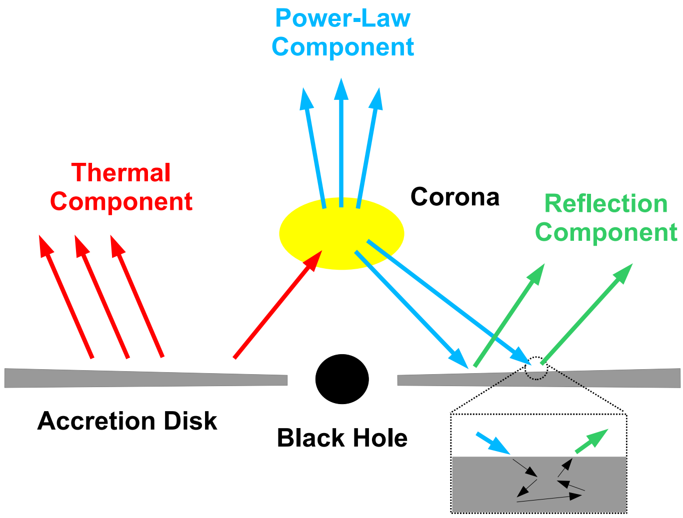

Figure 2. General scheme of a BH-XRB high energy emission region Bambi (2018).

In this type of systems, the compact object feeds on the strong stellar wind from its massive companion. This regime leads to persistent X-ray emission. Thus, this class of XRBs consists of persistently accreting BHs and X-ray pulsars (Walter et al. 2015).

A peculiar distinct subgroup of HMXBs is Be-XRBs (Reig 2011). Typically they consist of a NS and a Be star, a type of B-class star with a circumstellar decretion disk. These systems show periodic X-ray outbursts which occur when the NS passes through the circumstellar disk near the periastron around the Be-star. Between outbursts, Be-XRBs may go quiet or emit low-level X-rays.

1.2.2 Low mass X-ray binaries

In contrast, LMXBs pair a compact object with a lighter companion. These companions are typically much older, as the less massive stars can live for billions of years. As the part of the older population LMXBs are more often found in globular clusters or the galactic bulge (Gilfanov 2004). The companion star evolves slowly, stretching the lifespan of the whole system.

Mass transfer here usually happens through Roche lobe overflow, not stellar winds. As the companion star evolves it expands and can eventually fill its gravitational equipotential surface. This critical size depends on the binary separation and mass ratio. Once reached, stellar material flows through the inner Lagrangian point (L1) towards the compact object and forms the accretion disk.

These systems tend to be transient, with periods of quiescence interrupted by outbursts. LMXBs can also host both NSs and BHs. Their behavior will depend on which compact object is present. Some show unique features like X-ray bursts or rapid brightness changes.

A notable subclass of LMXBs are millisecond pulsars. So rapidly rotating NSs are thought to be spun up to hundreds of revolutions per second by accreting matter from their companions on the earlier stages of co-evolution (Bhattacharya & van den Heuvel 1991). During periods of accretion it exhibits millisecond X-ray pulsations formed by the funneled accrion onto its magnetic poles. When accretion stops, the system may become detectable as a radio millisecond pulsar.

1.3 Observational states and transitions

XRBs are observed in distinct spectral states where their spectra exhibit different relative brightness in different energy bands (Belloni 2010). Most generally, two main states are identified in XRBs: the hard state and the soft state. This distinction has been established since the *Uhuru* observation of spectral transition of one of the first and most studied BH-XRBs, Cygnus X-1 (Tananbaum et al. 1972), which primarily resides in the hard state but can transition to the soft state. In the hard state, the X-ray spectrum is dominated by a hard power-law component extending to high energies and little contribution from a thermal component. In the soft state, the X-ray spectrum is dominated by a strong thermal component, while the hard power-law component is much weaker. Historically, XRBs in the soft state exhibited higher flux in soft X-ray band than those in the hard state, which is why these states are often referred to as "high" and "low", respectively. However, the relationship between spectral shape, overall luminosity and time is different for different between classes of XRBs and then between different sources.

The physical interpretations for these spectral states involve changes in the accretion flow geometry and properties (Done et al. 2007). In the hard state, the accretion flow is believed to take the form of a hot, geometrically thick, radiatively inefficient accretion flow, often referred to as a "corona". The hard X-rays are thought to be produced by inverse Compton scattering off the hot electrons in the corona of soft photons from the disk or of synchrotron photons from the hot flow itself Poutanen & Vurm (2009); Nättilä (2024). In this state, the disk is truncated at a larger radius, and the inner regions are filled by the hot gas. The soft thermal emission is associated with a geometrically thin, optically thick, radiatively efficient accretion disk around the compact object. In the soft state, the thermal X-rays are emitted from the hot inner regions of the disk extended the very close vicinity of the compact object, while the corona is either absent or much weaker. Importantly, it is in the soft state that the accretion disk around a BH has a reasonably certain standard structure which helps infer the parameters of the BH. A similar description is expected to be valid for supermassive BHs, that is AGN, as well and may be connected with the difference between inactive and active galactic nucleus states (Blandford et al. 2019, section 3.1.2). However, as the timescales are orders of magnitude larger for them it is not yet viable to observe a transition between the states.

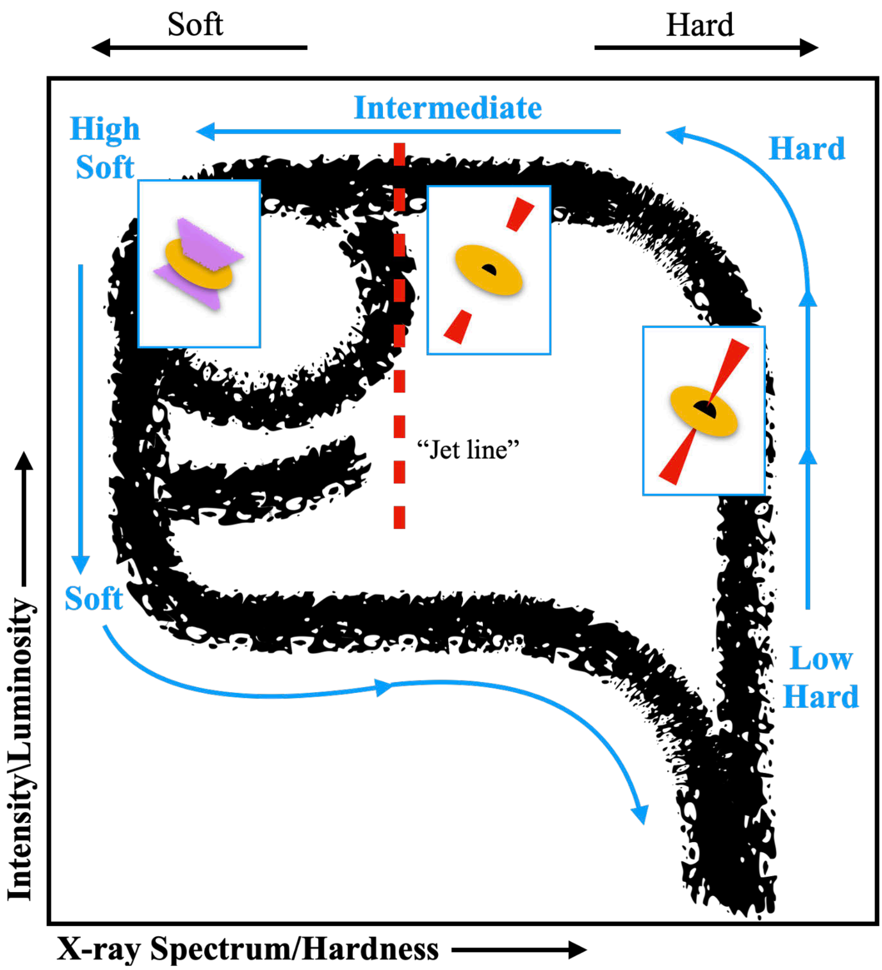

Figure 3. The schematic evolutionary track of an outburst of an XRB on the hardness-intensity diagram (HID) Moravec et al. (2022). The spectral states are labeled and the supposed underlying structures of the inner flows are shown.

The most typical behavior of an XRB is to exist in a quiescent state and experience typically weeks to months long outburst, during which it follows a letter Q-shaped trajectory on its HID. The typical sequence of the states and transitions is shown in Fig. 3. However, the XRBs are not resolved and the true structure of the accretion flow is never determined decisively. Instead, the only qualities we observe are the electro-magnetic (EM) spectrum and the light curve, which can also be analyzed through its Fourier spectrum. The X-ray spectrum features can often be fitted with different models, and the nature of different timing properties in X-ray brightness is also debated. A promising source of additional information about the X-ray bright flows around compact objects has always been the X-ray polarization features.

2 X-ray polarimetry

Astrophysicists are polarized on the issue of black hole spins, but luckily, X-rays are also polarized to set the record straight.

The significance of polarization measurements in astrophysics is highlighted by decades of theoretical research and modeling of polarization of X-ray radiation across various classes of astrophysical sources and exclusive information concealed in it. In the early motivation by Novick (1975), the potential of X-ray polarimetry was noted for the ability it has to provide insights into the geometry and emission mechanisms of astrophysical sources, including X-ray pulsars and solar flares. The critical role of polarization observations was further recognized over the years for almost all types of X-ray sources, investigating pulse profiles of rotation-powered and accretion-powered pulsars, identification of black hole candidates, probing the physical processes in supernova remnants, accretion disks, jets/blazars, Seyfert 2 galaxies (see Meszaros et al. 1988; Kallman 2004). Similarly, Krawczynski et al. (2011) covered the specifics of hard X-ray (>10 keV) polarization observations and its complementary nature to soft X-ray polarization observations of microquasars, AGN, and gamma-ray bursts.

2.1 Fundamentals of polarization

In general, polarization describes the geometric orientation of the electric field vector as an EM wave propagates through space. According to the general solution of the Maxwell equations considering an electromagnetic wave in a vacuum, the electric field vector traces out a regular ellipse in the plane perpendicular to photon propagation. This general elliptical polarization can be decomposed in terms of two primary modes: linear and circular components. The latter component, circular polarization, mainly emerges in very highly magnetized media and therefore it is less common and is also harder to detect, especially for X-ray wavelengths. For that reason, the research often focuses on the former, linearly polarized EM waves, which oscillate in a particular plane. The plane of oscillation for a linearly polarized photon has an arbitrary orientation orthogonal to the direction of photon propagation. Furthermore, light is generally an incoherent superposition of multiple polarized wave components. The fraction of the total intensity polarized along the predominant polarization plane is described by the polarization degree (PD). The orientation of this plane is described, in turn, by the polarization angle (PA), the position angle around the line of sight of the observer, relative to a reference direction.

A convenient way to represent polarization is through the Stokes parameters, formulated by Sir George Gabriel Stokes in 1852. The Stokes vector has four components:

- I represents the total intensity of the light, regardless of polarization;
- Q is the difference in intensity between horizontally and vertically polarized light;
- U is the difference between polarizations at 45° and −45°;
- V is, lastly, the difference between left- and right-circularly polarized light (that is clockwise and counterclockwise).

The Stokes vectors are useful because, unlike the undirected pseudovector of polarization, they mathematically behave like vectors. They transform regularly under coordinate rotations and they can be summed together for polarized radiation from multiple incoherent sources. Unpolarized radiation has

$$Q = U = V = 0 \tag{1}$$

while 100% polarized radiation has

$$I^2 = Q^2 + U^2 + V^2. \tag{2}$$

The PD is given by

$$p = \frac{\sqrt{Q^2 + U^2 + V^2}}{I}. \tag{3}$$

In X-ray astrophysics the circular polarization is often omitted from consideration, as there is not yet a possibility to measure circularly polarized X-ray photons. The PA of linear polarization is simply half of the angle that the Stokes vector makes on the Q–U plane. The degree of linear polarization corresponds to how far away the Stokes vector is from the origin:

$$p = \frac{\sqrt{Q^2 + U^2}}{I}, \tag{4}$$

normalized by the total intensity. The PA is typically defined over a 180-degree range either from 0° to 180° or from −90° to 90° since the polarizations rotated by 180° to each other are equivalent. And it can be defined as

$$\chi = \frac{1}{2}\arg(Q + iU) = \arctan\left(\frac{pI - Q}{U}\right). \tag{5}$$

Viewing the data in different polarization representations can reveal effects that may not be obvious otherwise. It can be useful to look at both the natural PA and PD parameters, as well as visualizing the evolution of the Stokes Q and U parameters on the Q–U plane, when studying how the polarization changes over time for an astronomical source. The Stokes vectors add together linearly. It is helpful for identifying potentially separate components of polarized emission. For example, as showcased in Doroshenko et al. (2023), the pulsar exhibits some unanticipated periodicity in its polarization angle parameter (illustrated in the Fig. 4). On the Q-U plane, it may become clear that in addition to the typical polarization variability from the pulsar itself, there is an extra constant polarized component present from another astrophysical mechanism. In that case, the phase-dependent data points will sweep similar shapes on the plane, while the PD and PA profiles may look drastically different (see more in Poutanen et al. 2024).

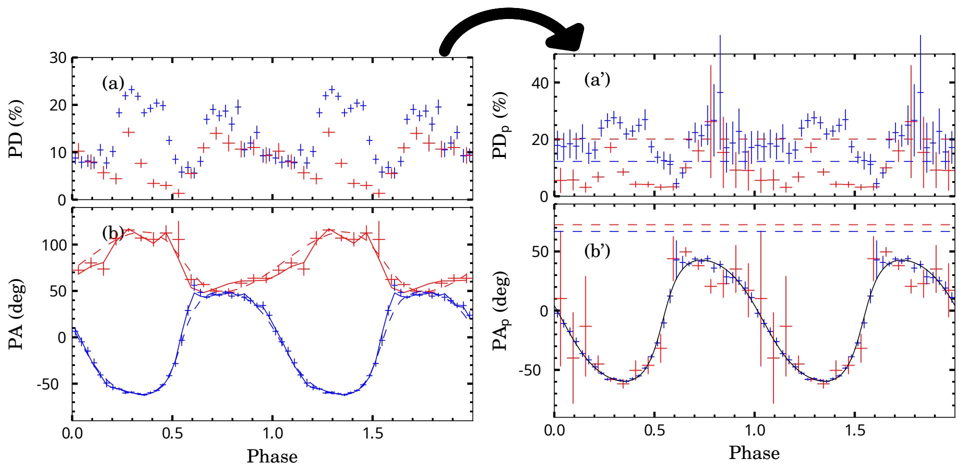

Figure 4. The figure is combined from Figures 3 and 6 in Doroshenko et al. (2023). The left one shows the rotating vector model fit of the two observations separately, and the right shows the simultaneous fit after introducing a constant polarized component.

2.2 X-ray polarization

As mentioned before, polarization is a property of light regardless of the wavelength. In X-rays, polarization was confirmed only several years after the discovery of this emission, so it was natural for scientists to assume that X-rays, like any other light, can become polarized. The key difference between X-ray and, for example, visual light polarization is in the mechanisms responsible for the appearance of the preferred polarization direction. As both mechanisms of creating the X-ray emission and the ways it interacts with the matter are unique for the X-ray light, the polarimetric properties of the X-ray emission contain distinctive information about a source.

Polarimetric properties of the light coming from a distant source depend strongly on the mechanisms of emission and acceleration of the particles and source geometry, including the magnetic field geometry and strength. As X-rays are emitted from compact objects, this light is produced and propagated in the extreme gravitational and magnetic fields that we are unable to reproduce in laboratories on Earth. Hence, polarized X-rays also provide information about the geometry and emission processes near these objects.

2.2.1 Thomson Scattering

Thomson scattering, named after the British physicist J.J. Thomson, is one of the most basic mechanisms for X-ray polarization in astrophysical contexts. It is defined as the scattering of photons by free charged particles, typically electrons, in the classical limit where the photon energy is much less than the rest mass energy of the particle. The cross-section for Thomson scattering is independent of the photon wavelength and the wavelength of the scattered radiation also remains unchanged. The scattered radiation becomes polarized, with the PD depending on the scattering angle. The PD as a function of scattering angle is given by

$$p(\theta) = \frac{1 - \cos^2\theta}{1 + \cos^2\theta}, \tag{6}$$

where θ is the scattering angle. Maximum polarization occurs for scattering angles of $90°$.

The detailed mathematical formalism for Thomson scattering was described in the formative work by Chandrasekhar (1960). One notable and important result derived there is for radiation emerging from an optically thick, electron-scattering dominated atmosphere. The maximum PD of $\approx 11.7\%$ can be achieved when viewed edge-on. This limit often serves as a benchmark in interpreting observed polarization levels.

Thomson scattering typically plays a role as the primary mechanism for generating polarization in low-energy regimes, such as NS atmospheres, cold accretion disks or stellar winds. The scattered photons can become polarized, especially if the scattering occurs in a non-spherically symmetric environment. Basically, if the surface of the emitting medium is viewed edge-on, the X-rays can show a higher degree of linear polarization. Thomson scattering is particularly useful for probing the geometry of the accretion flow and the orientation of the binary system.

2.2.2 Compton Scattering

In high-energy environments, Compton scattering is often the main contribution to polarization. In principle, Compton scattering is equivalent to Thomson scattering but includes the quantum and special relativity (SR) effects. The direct Compton effect is observed when the scattered photon possesses energy comparable to the rest-mass of the particle it is scattering off (511 keV for an electron). In that case, the energy of the photon is enough to increase the momentum of the particle, therefore there is a decrease in the photon frequency. In the opposite case, a photon will gain energy by scattering off a much more energetic electron. This process is much more common in astrophysical environments and is called inverse Compton scattering (see White et al. 1988, and references therein). Similarly to the Thomson case, the scattered photons are polarized, and the PD varies with the scattering angle of the photon. Additionally, the change in energies of the particle will also depend on the scattering angle. An exhaustive physical and mathematical description of the process is given in the review by Nagirner & Poutanen (1994). This process is relevant in the "corona" around the accretion disk, where hot electrons energized by plasma effects can upscatter photons from the disk to higher energies. Similarly, the Compton scattering dominates parts of the spectra of accreting NSs, where the electrons of the hot accreted matter upscatter the radiation from the NS surface.

2.2.3 Synchrotron Radiation

In systems with strong magnetic fields, especially those involving neutron stars, synchrotron radiation can be a significant source of polarized emission. Charged particles spiraling along magnetic field lines emit synchrotron radiation that is highly polarized. The degree and orientation of the polarization can provide direct information about the configuration of the magnetic fields. This is particularly relevant in systems where jets are present, as the jets are often thought to be launched along magnetic field lines.

The simplest and the most widely used relation is for the PD of synchrotron radiation

$$p = \frac{\alpha + 1}{\alpha + 7/3} \tag{7}$$

of leptons with power law energy distribution, $N \propto E^{-\alpha}$, derived in Le Roux (1961); Legg & Westfold (1968). This becomes increasingly important for observations of blazars and pulsar wind nebulae, where the radiation is dominated by relativistic electrons in strong magnetic fields.

Among other sources of polarized emission, one can mention also vacuum polarization arising in presence of powerful magnetic fields, typical for highly magnetized X-ray pulsars (Mushtukov et al. 2018). As these objects do not appear in the research presented in this work, they are left without a detailed description.

2.3 IXPE and X-ray polarimetry

As instruments specifically designed for polarimetric studies in other energy ranges had already proven themselves invaluable (see more in Section 2.4), it was only natural for X-ray polarimetry to join the club. The papers presented in this thesis are motivated by the launch of *IXPE* in 2021 or based on the most recent results of this mission. Similarly to the previous (unsuccessful) projects of the instruments dedicated fully to X-ray polarimetry, *IXPE* brought a new wave of interest and hope to the field.

X-ray polarimetry had a thorny way to the important place it occupies now as one of the very promising tools to unravel the mysteries of the X-ray universe. This challenging, demanding, and sometimes exhausting journey is first-hand reviewed in great detail by Weisskopf (2018). The most contemporary comprehensive review of the history of X-ray polarimetry including the *IXPE* era is given by Costa (2024).

2.3.1 Historical missions

Since the confirmation of the polarization in the X-ray in the beginning of 20th century (Barkla 1904), it took scientists almost 65 years to obtain the first measurements of the X-ray polarization from outside the Solar system. The first polarimeter was launched on board the sounding rocket in 1968 by a group from Columbia University (Novick & Wolff 1971). The aim was to measure the polarization of the weakly magnetized neutron star Sco X-1 and the Crab Nebula. Unfortunately, the lithium scattering polarimeter was not able to make a detection, and only the upper limit of 20% PD for the Crab Nebula was derived from the data (Novick et al. 1971). After adding four mosaic graphite crystal Bragg polarimeters to the lithium scattering polarimeter for the second sounding rocket experiment, the results improved significantly. This time, the rocket was observing the Crab Nebula, and the science team managed to detect a PD of $15\% \pm 5\%$ at a PA of $156° \pm 10°$ (Novick et al. 1972).

The next step in developing X-ray polarimetry was the launch of Orbiting Solar Observatory (OSO-8) (Mitchell et al. 1976). OSO-8 also observed the Crab Nebula and improved the measurements of the polarization of the Crab Nebula to the PD of $19\% \pm 1\%$ and the PA of $156.4° \pm 1.4°$ (Weisskopf et al. 1978). Two graphite crystal polarimeters on board OSO-8 were mainly able to provide upper limits for the PD of the sources it observed, but it also made marginal detections of the polarization of the black-hole XRB Cyg X-1 and a weakly magnetized neutron star Cyg X-2 (Long et al. 1980).

Ariel V, another mission launched in the seventies, had a Bragg crystal spectrometer/polarimeter on board (Smith & Courtier 1976). Its only polarimetric results were an upper limit on the polarization of Sco X-1 (Gowen et al. 1977) and the absence of linear polarization in the X-ray from BH-XRB A0620−00 (Griffiths et al. 1976).

The next project, Stellar X-ray Polarimeter (SXRP), meant to include both a Bragg crystal scattering polarimeter and a newly developed photoemission polarimeter (Kaaret et al. 1990). The instrument was to be placed on a slide to occasionally put it at the focus of an X-ray telescope aboard the Soviet mission Spectrum Roentgen-Gamma. The mission was planned to be launched in 1987 but was postponed several times due to the fall of the Soviet Union, and was eventually canceled. The mission bearing the same name was ultimately launched without a polarimeter (Sunyaev et al. 2021). This project, however, gave rise to a new wave of interest in X-ray polarimetry.

2.3.2 IXPE

IXPE was launched on 2021 December 9 to specifically study the polarization of X-rays emitted by various cosmic sources. A joint project of the National Aeronautics and Space Agency (NASA) and the Italian Space Agency, it required the efforts of hundreds of scientists from all over the world and decades of engineering advancements to become the success it is now. The observatory itself consists of three identical grazing incidence telescopes. Each telescope comprises an X-ray mirror assembly and a polarization-sensitive detector unit (DU) equipped with a gas-pixel detector (Baldini et al. 2021). The new polarization detection technique is based on the photoelectric effect and the dependence of the direction of photo-electron ejection on photon polarization. The gas-pixel detectors are capable of tracing the photoelectron motion in the detector, providing an image of the photoelectron track. The polarization is then determined by the distribution of the photoelectron azimuthal directions. This architecture allows for a much more precise and time-sesitive polarization measurement of X-ray polarization than the previous missions. Overall, *IXPE* provides imaging polarimetry over the 2–8 keV energy band with a time resolution of the order of 10 μs. A detailed description of the observatory and its performance is given in Weisskopf et al. (2022) and the observatory itself is depicted in Fig. 5.

In the first two years of operation, *IXPE* managed to observe several dozens of sources, among which are AGN, microquasars, pulsars and pulsar wind nebulae, magnetars, XRBs, supernova remnants, the Galactic center, and even the gamma-ray burst (GRB) afterglow. *IXPE* has been extended beyond the original two-year operations and is currently in the stage of the General Observer (GO) program.

The future is promising with upcoming missions and advancements in detector technology that will allow for more precise and comprehensive studies of X-ray polarization in various astrophysical contexts. New missions (e.g. *eXTP* Zhang et al. 2019; *REDSoX* Heine et al. 2024), as well as new approaches (e.g. 3-Dimensional photoelectron track reconstruction, see Kim et al. 2024), are being developed. X-ray polarimetry has shed new light on many high-energy phenomena, yet it has more to offer to the scientific community.

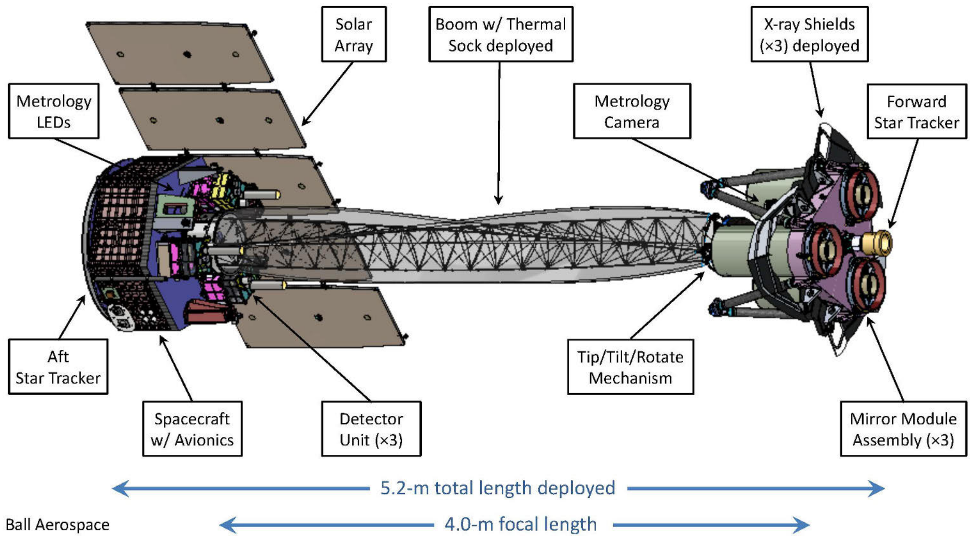

Figure 5. The outline of the *IXPE* observatory architecture. From Weisskopf (2018)

2.4 Some multi-wavelength polarimetry

It is not only the X-rays that are capable of providing new discoveries in compact objects. Studying polarization across different wavelengths provides an even more comprehensive view of the physical processes in high-energy astrophysical systems.

High precision polarimetry (Berdyugin et al. 2019) has somewhat limited but important results for XRBs (Kravtsov et al. 2022). In particular, one noteworthy result is the discovery of a high ($> 40^\circ$) misalignment between the black-hole spin and the orbital axis in XRB MAXI J1820+070 (Poutanen et al. 2022).

On the other side across the X-ray band, in γ-rays, there have been attempts to measure the polarization in power-law tail part of the spectrum of XRBs. In particular, INTEGRAL (INTErnational Gamma-Ray Astrophysics Laboratory) has provided high PD estimates of several sources. For example, high γ-ray polarization was detected independently for CygX-1 with instruments onboard INTEGRAL: $67 \pm 30\%$ at $0.4 - 2$ MeV with the imaging instrument, IBIS, (Laurent et al. 2011) and $> 76\%$ above 230keV with the spectrometer, SPI, (Jourdain et al. 2012). However, the PA measured in both cases was $\sim 60^\circ$ away from the direction of the compact radio jet and the polarization measured in the other bands, which is puzzling. Lately, CZTI instrument onboard AstroSat (with extended energy range with Compton spectroscopy) detected significant $23 \pm 4\%$ polarization of Cyg X-1 in hard intermediate state in $175 - 380$ keV range (Chattopadhyay et al. 2024) with the PA roughly 90° away from one measured in soft X-rays by *IXPE*. This highly polarized γ-ray emission can be associated to synchrotron self-Compton (SSC) of high-energy electrons in the jet and may be a hint of a distinct spectral component at higher energies in the source. Alternatively, the detections can be false, as the instruments were not initially designed and calibrated for γ-ray polarimetry.

3 Ray-tracing techniques in curved spacetimes

As X-rays reach far from their source, so do your deeds stretch into eternity.

Compact objects are termed "compact" because their gravitational radius is not significantly smaller than their actual radius. The study of compact objects such as NSs and BHs requires comprehension of general relativity (GR) and the curvature of spacetime. For instance, a typical NS with a mass of 1.4 times that of the Sun and a radius of around 12 kilometers has a gravitational radius of only about a fifth of its actual size. Thus the extreme density and gravitational pull of the star affects both the sophisticated physics of its interior and the appearance of its surface, where most of the observable radiation is coming from. BHs, on the other hand, demonstrate the absolute extreme case of compactness where the event horizon resides at the Schwarzschild radius, that is twice the gravitational radius, for a non-rotating BH, and down to just one gravitational radius for extremely rotating BHs. Although the surface of a BH does not exist and the event horizon does not emit light, the accretion disk surrounding it, according to standard models, reaches peak brightness near to the BH, specifically four to five Schwarzschild radii if the orbit of the disk aligns with the rotation of the BH.

The positioning of the emitting matter at the gravitational scales of the compact object complicates the process of decoding the astrophysical aspects of these systems, particularly their observed geometry, observed through curved light paths. The light does not travel in straight lines near these objects because it follows the curvature of spacetime created by their gravity as predicted by Einstein's theory of GR, leading to phenomena such as gravitational lensing. Understanding and taking these effects into account is necessary for interpreting the observational data accurately. When analyzing the polarization parameters of light from around compact objects, the effects of relativity become particularly important as the effects are exactly geometrical. In chapter 1 we discussed the general observational properties of compact objects within X-ray binaries, and the main physical processes that occur in these systems, In this chapter, we will focus on the particular aspects and properties of the spacetime around compact objects, and methods to study the behavior of light and matter in the curved spacetime.

3.1 Astrophysical compact objects and spacetime solutions

NSs and stellar mass BHs share several observational aspects, including their influence on surrounding matter and their role in emitting and lensing of high-energy radiation. In the case of moderately spinning NSs, their lensing properties can be approximated by a central singularity. In other words, the formalism for lensing by a BH discussed below is also widely applicable to most NSs. For rapidly rotating ones, not only is the spacetime affected by the angular momentum but also, and often even more so by the non-spherical mass density distribution due to the centrifugal forces (see AlGendy & Morsink 2014). This emphasizes the importance of modeling the numerical spacetime solutions for NSs and ray-tracing through them.

Stellar BHs formed from the remnants of massive stars typically have masses ranging from about three to tens of solar masses. Observations of these objects are often detected through the X-ray emissions from accreted matter in binary systems, because single stellar mass BHs are unable to accrete enough interstellar matter to sustain an observable accretion flow. However, it is possible to discover a wandering BH by the gravitational lensing of a background star.

In contrast to BHs formed from stellar remnants, supermassive BHs reside at the centers of galaxies, including our own Milky Way. These BHs have masses that can be billions of times that of our Sun, accounting for a significant fraction (up to several per cent) of the stellar mass of their host galaxy (Kormendy & Ho 2013; Bentz & Manne-Nicholas 2018). The origins of supermassive BHs are a subject of ongoing research and debate (Volonteri 2010), yet their existence is unquestioned. Thus they provide opportunities to observe extreme physics of BH accretion not just in our galaxy but also in distant galaxies. Supermassive BHs play a central role in the phenomenon of AGN, where they accrete matter from their surroundings and emit radiation across a broad spectrum, from radio wavelengths to gamma rays.

The distinction between stellar-mass BHs and supermassive BHs is not just quantitative mass differences. Indeed, the mass gap between these two classes is very broad, and only a handful of candidates for intermediate-mass BHs have been identified (Miller & Colbert 2004; Greene et al. 2020). These different types of BHs are often studied by different communities of astrophysicists due to the drastic distinction between these phenomena. One difference lies in the nature of accretion. Galactic BHs, or stellar-mass BHs, typically accrue mass from a companion star, whereas supermassive BHs at the centers of galaxies are often solitary accreting mass from the surrounding interstellar medium and stars. Furthermore, binary galactic cores have been discovered (Goulding et al. 2019), although it is not about accretion from a companion. Furthermore, the observational timescales vary dramatically due to their mass differences and therefore the difference in the dynamic timescales of processes around the BHs. For instance, quasi-periodic oscillations in stellar-mass BHs are measured in Hz (see e.g. Ingram & Motta 2019), while in quasars and Seyfert galaxies, which host supermassive BHs, similar phenomena may span days and years (see e.g. Ren et al. 2023, and references).

Nonetheless, from the standpoint of radiation transfer and light bending, the mass of a BH does not mathematically alter the fundamental behavior of spacetime curvature around it. According to the general theory of relativity, the spacetime curvature behaves similarly around both supermassive and stellar-mass BHs in proportion to the gravitational radii. This implies that solutions to ray tracing problems, which predict the paths of light in the curved spacetime near BHs, are equally applicable and beneficial for probing the environments around BHs of both classes.

3.2 Schwarzschild metric

According to the no-hair theorem, a BH in general relativity is completely characterized by only three properties: mass, charge, and angular momentum (Misner et al. 1973). The Schwarzschild metric describes a BH with only mass with no other properties. The Schwarzschild metric is the simplest and most well-known solution to Einstein's field equations of general relativity, describing the gravitational field outside a spherically symmetric (or point-like, that is a singularity), non-rotating, uncharged mass. It was derived by Karl Schwarzschild (1916), shortly after Einstein's publication of the general theory of relativity.

The Schwarzschild metric is given by the line element:

$$ds^2 = -(1 - 2M/r)dt^2 + (1 - 2M/r)^{-1}dr^2 + r^2(d\theta^2 + \sin^2\theta d\phi^2), \tag{8}$$

where:

- M is the gravitational mass of the central object,
- r is is the circumferential radius,
- t is the time coordinate,
- and θ and ϕ are the angular coordinates.

The event horizon is the surface around the singularity from beyond which neither matter nor information can escape. Physically, this also corresponds to the boundary, where the escape velocity exceeds the speed of light. It is located at a radial distance of $r = r_{\rm S} = 2GM/c^2$ ($r = 2M$ in natural units where $G = c = 1$), known as the Schwarzschild radius. Thus, the event horizon is a perfect sphere in the Schwarzschild case, and the spacetime is also spherically symmetric.

The Schwarzschild solution predicts how light rays will be deflected by the gravitational field of a massive object. This phenomenon, referred also as gravitational lensing, is responsible for the events when light from distant sources is deflected by the gravitational field of massive objects, creating multiple images, arcs, or rings. In the case of XRBs, lensing largely affects the appearence of X-ray emitting regions, as has been discussed earlier. We can observe the opposite side of an accretion disk through the opening in its center. This is also responsible for the fact that we see more than half of the surface of a NS, of course if it is not occluded by anything else. Qualitatively, the effect of lensing can be approximated with the Schwarzschild metric.

In the Schwarzschild metric, light rays follow planar trajectories, confined to a single plane passing through the center of the mass. Thus, the geodesics are defined as single variable functions and this allows for a simple analytical solution for the light bending. If the photon is emitted at a distance R from the center of the mass, at an azimuthal angle α to the radial direction, in the plane of the geodesic, the deflection angle ψ at infinity can be computed simply with integral expression (Misner et al. 1973; Beloborodov 2002):

$$\psi = \int_R^\infty \frac{dr}{r^2}\left[\frac{1}{b^2} - \frac{1}{r^2}\left(1 - \frac{r_\mathrm{S}}{r}\right)\right]^{-1/2}, \tag{9}$$

where b is the impact parameter

$$b = \frac{R}{\sqrt{1-u}}\sin\alpha. \tag{10}$$

This integral can be computed numerically with relative ease after a substitution. However, an extremely simple approximation can be made for the deflection angle, (Beloborodov 2002):

$$1 - \cos\alpha \approx (1 - r_\mathrm{S}/R)(1 - \cos\psi), \tag{11}$$

which is valid relatively well for the a decent range of impact parameters and angles. An improvement for this analytical approximation was introduced by Poutanen (2020). With addition of a few more terms, the approximation covers angles almost all the way up to 180° and the accuracy is improved down to 0.2% for the bending angle. This practically removes any need to compute numerically the integral along the geodesic in most astrophysical problems. In particular, one does not have to follow the continuous evolution of the polarization vector along the geodesic, because the polarization vector of every photon is transported parallel along the geodesic keeping its angle to the plane of the trajectory. This makes it particularly straightforward to compute polarization rotation due to GR effects. We make use of this property in the technique described in paper I for NSs and then in paper IV for BHs.

3.3 Kerr metric

The Kerr metric is an exact solution to Einstein's field equations describing the curved spacetime geometry around a rotating, uncharged BH. It was derived by the New Zealand mathematician Roy Kerr (1963). The Kerr metric generalizes the static, spherically symmetric Schwarzschild solution to the case of a rotating mass with angular momentum.

While originally obtained for spinning BHs, the Kerr metric could be a good approximation for the exterior spacetime around a rotating, axisymmetric mass distribution, such as rapidly spinning NSs like millisecond pulsars. However, for such realistic compact objects containing matter, the spacetime differs from Kerr spacetime due to mass distribution and especially rotational effects like oblateness from centrifugal forces. In general, numerical solutions or simulations are required to fully model the interior and exterior spacetime (Hartle & Thorne 1968; Friedman et al. 1986; Miller et al. 1998; Yagi & Yunes 2013; AlGendy & Morsink 2014). Nevertheless, the Kerr metric remains a benchmark solution for the physics around rotating BHs and other highly compact, rapidly spinning astrophysical objects.

A spinning Kerr BH is non-spherical and exhibits some phenomena that are not present in the static Schwarzschild solution. In addition to the typical event horizon boundary, the Kerr solution exhibits an "ergosphere" region between the outer event horizon and a more inner "static limit" surface. Within this ergosphere, any physical object must co-rotate with the spinning spacetime geometry of the BH due to intense "frame-dragging" effects. However, unlike the event horizon, light and particles can still escape from the ergosphere.

Another distinctive and important feature is that the innermost stable circular orbit (ISCO) for particles and accretion disks depends on the normalized spin parameter of the BH, $a = Jc/GM^2$, where J is the angular momentum of the BH, so the spin is defined between -1 and 1. The ISCO radius is (see e.g. Kato et al. 2008)

$$r_{\mathrm{ISCO}} = \frac{1}{2}\left(3 + Z_2 \pm \sqrt{(3 - Z_1)(3 + Z_1 + 2Z_2)}\right), \tag{12}$$

where the minus sign gives the value for the co-rotating particle and the plus sign is for the retrograde particles, and:

$$Z_1 = 1 + \sqrt[3]{1 - a^2}\left(\sqrt[3]{1 + a} + \sqrt[3]{1 - a}\right), \tag{13}$$

$$Z_2 = \sqrt{3a^2 + Z_1^2}. \tag{14}$$

Inside the ISCO radius, no stable orbits are possible, so accretion disk emission originates only from larger radii. Since the ISCO radius depends on spin, analysis of the spectral features of the dick can reveal the angular momentum of the central compact object.

Thus, the Kerr metric solution has enabled analytic models of accretion disks around rotating BHs. One of the seminal works in this area is the standard thin disk model developed by Novikov & Thorne (1973). Their model treats the accreting gas as a steady-state, axisymmetric, multi-temperature blackbody disk following circular geodesic orbits described by the Kerr geometry. By applying the laws of conservation of rest mass, energy, and angular momentum, along with the Reynolds conditions and vertical hydrostatic equilibrium, they derive the radial structure of such a disk. The Novikov-Thorne model predicts the radial profiles of disk quantities like the radiative flux, temperature distribution, and emission spectra as a function of the BH spin parameter. While simplified, this analytic model has remained an important tool for interpreting observations of accretion disks and extracting spin estimates for rotating BHs. More sophisticated numerical simulations now exist, but the Novikov-Thorne disk model still provides a foundational framework for accretion onto rotating Kerr BHs using the basic principles of GR, hydrodynamics and radiative transfer.

3.4 Ray-tracing

Unlike the static Schwarzschild geometry, the dragging of inertial frames around a spinning point mass causes geodesics to be non-planar. This makes it even more challenging to compute the observed parameters analytically. Although some analytical expressions can be written down for a subset of specific cases (see e.g. in Li et al. 2009; Dexter & Agol 2009), the fully analytical approach is lengthy and not transformable enough for effective inference of accretion flow parameters in Kerr spacetime. It becomes even more difficult when the body cannot be considered as a point mass, for instance, a rapidly spinning NS becomes oblate under the influence of its own rotation. The same can be said when more than one massive body is considered, which is a natural scenario for electromagnetic counterpart for gravitational waves from a merger of a close binary of compact objects (although the pre-merger EM counterpart is not expected to be observed in a foreseeable perspective). Finally, when alternative spacetimes are considered to test general relativity (see e.g. Johannsen & Psaltis 2011), the go-to approach is purely numerical techniques which remove the necessity to derive analytic formulas for metrics with many parameters. In all these instances the geodesics will have to be numerically simulated and this process is called ray-tracing.

3.4.1 Polarized ray-tracing approaches

Generally, two basic ray-tracing schemes can be distinguished based on the direction of geodesic solution extrapolation:

- Forward ray tracing from the object to the observer. The virtual photons are emitted from the surface of the object in all possible different directions. With a large enough sample size of this Monte-Carlo simulation reaches enough statistics to build the observed spectro-polarimetric appearance of the object for a range of observers at infinity. Examples of codes that implement this approach include, among others, `grmonty` (Dolence et al. 2009), `xTrack` (Krawczynski 2012) and `Pandurata` (Schnittman & Krolik 2013). This approach is especially convenient for a complex emitter, such as a numerical hydrodynamic simulation with values only directly available on a given grid. The downside of this approach is usually the fact that Monte-Carlo simulations tend to be very noisy and require simulating a very large quantity of virtual particles to gather a decent statistics and even more so for polarized light, especially when the PD is not very high.

- Backward ray tracing from the observer to the object. Geodesics stretch out from a numerical observer towards the object in question (backwards in time) until they hit the emitting surface, defining the emission parameters (the emission angle, the intensity, polarization parameters and so on). Noteworthy codes that exemplify this scheme include `geokerr` (Dexter & Agol 2009) and ARCMANCER (Pihajoki et al. 2018). This approach is more convenient for imaging, as it gives straightforward control over the image plane grid. On the other hand it is hard to predict the point where at the emitter a given photon lands.

Either way, building a comprehensive model of the emission of a compact relativistic object will require computation of a large amount of light rays, and many such models (such as Krawczynski & Beheshtipour 2022) therefore must rely on the pre-computed arrays of geodesics for the whole parameter space of a given problem (e.g the spin of the BH, the inclination of the disk, and so on).

3.4.2 Basics of ray-tracing

In GR, spacetime is described as a four-dimensional Lorentzian manifold, where the gravitational interaction manifests itself through the curvature of this manifold. The main object characterizing the geometry of spacetime is the metric tensor $g_{\mu\nu}$. It describes the intervals between events (distances and time intervals) and determines the trajectories of particles and light. The metric tensor defines the interval ds between two infinitely close events by

$$ds^2 = g_{\mu\nu} dx^\mu dx^\nu, \tag{15}$$

where dx^μ and dx^ν - are coordinate differentials. For different astrophysical objects there are specific forms of the metric tensor reflecting their gravitational fields. Some are possible to obtain analytically from the Einstein field equations, and some have to be approximated numerically.

To further illustrate this concept, consider the Kerr spacetime, which is used to describe a rotating astrophysical BH. This spacetime solution has only two parameters: the mass M and the spin a. The Kerr metric can be expressed in different coordinate systems. The most common is the generalization of "spherical" coordinates used for Schwarzschild BHs, the Boyer–Lindquist (BL) coordinates $(t,\ r,\ \theta,\ \phi)$, which are reduced to Schwarzschild coordinates when the spin parameter $a = 0$. The metric tensor in this system takes the form

$$g_{\alpha\beta} = \begin{pmatrix} 1-\frac{2Mr}{\rho^2} & 0 & 0 & \frac{2Mra\sin^2\theta}{\rho^2} \\ 0 & -\frac{\rho^2}{\Delta} & 0 & 0 \\ 0 & 0 & -\rho^2 & 0 \\ \frac{2Mra\sin^2\theta}{\rho^2} & 0 & 0 & -\sin^2\theta\left(r^2+a^2+\frac{2Mra^2\sin^2\theta}{\rho^2}\right) \end{pmatrix}, \tag{16}$$

where $\Delta = r^2 - 2Mr + a^2$ and $\rho^2 = r^2 + a^2\cos^2\theta$. However, different coordinate systems can be used to describe the same spacetime solution, for example, Kerr-Shild coordinates $(t,\ x,\ y,\ z)$, proposed later by Roy Kerr and Alfred Schild, describe the same spacetime shape but in a Cartesian-like way. To express the curvature of a spacetime in given coordinates the Christoffel symbols (Γ) are used. They are defined through the metric tensor and derivatives of its components in a given coordinate system:

$$\Gamma^{\alpha}_{\mu\nu} = \frac{1}{2}g^{\alpha\rho}(\partial_\mu g_{\nu\rho} + \partial_\nu g_{\mu\rho} - \partial_\rho g_{\mu\nu})\,. \tag{17}$$

A ray-tracing technique boils down to solving the geodesic equation numerically. The geodesic equation is written as second order partial differential equation

$$\frac{\mathrm{d}^2 x^\alpha}{\mathrm{d}\lambda^2} + \Gamma^{\alpha}_{\mu\nu}\frac{\mathrm{d}x^\mu}{\mathrm{d}\lambda}\frac{\mathrm{d}x^\nu}{\mathrm{d}\lambda} = 0\,, \tag{18}$$

which describes a parametric curve of the particle coordinates x^α along the parameter λ, which is the proper time in the case of a massive particle or the affine parameter for a massless particle (in which case it is called a null geodesic).

Then the unit polarization vector f^α must be transported along the geodesic so that it is satisfied the parallel transport equation

$$k^\alpha \nabla_\alpha f^\beta = 0, \tag{19}$$

which equation ensures that the polarization vector remains orthogonal to the wave vector $k^\alpha = \frac{\mathrm{d}x^\alpha}{\mathrm{d}\lambda}$ along the entire geodesic, that is $k_\alpha f^\alpha = 0$. In the Schwarzschild spacetime, where the geodesics are planar, the parallel transport of the polarization vector is straightforward, as the polarization vector conserves the angle to the plane of the trajectory. In this simple case, computing the GR effects on the polarization is no different from computing the effects of SR or the geometry of the emission region. We rely on this property in our derivations in paper I, paper IV, and paper V.

4 Future prospects

An oblate brightly flashing object
can be called an epilepsoid.

With the *IXPE* mission, the era of X-ray polarimetry has just started and the amount of new questions the first observations posed for high-energy astrophysics community outweighed the problems they helped to solve. For example, in X-ray pulsars, where the phase resolved polarization was expected to reach high values up to 80%, the observed polarization turned out to be much lower (see e.g. Doroshenko et al. 2022a). On the contrary, for BH-XRBs in many cases, the values of polarization degree exceeded the most optimistic expectations (see e.g. Krawczynski et al. 2022; Ratheesh et al. 2024). The accurate models of the accretion flows around the compact object are yet to be discovered. The work towards this goal is already going, facilitated by the quickly expanding pool of new observational data.

4.1 Accreting Millisecond Pulsars

Accreting millisecond pulsars (AMPs) are a favorable class of objects for X-ray polarization spectroscopy and timing. The first object of this class observed with *IXPE* is SRGA J144459.2−604207, but the data did not allow for a detection of expected variability of polarization parameters over the pulse phase. Another promising source, SAX J1808.4−3658, is the prime candidate for prospective *IXPE* observations, being the only AMP that goes into outburst regularly and is bright enough for *IXPE* to detect. The observation of polarization properties of the next outburst of SAX J1808.4−3658 with *IXPE* will provide an opportunity to constrain its geometrical configuration and accretion structure, building upon the results of previous NICER observations (Bult et al. 2019) as well as simultaneous observations. This will allow for a more comprehensive understanding of the emission mechanisms and geometry of the source and AMPs in general.

The observation and accumulation of statistics on AMPs as a class is a highly desirable research direction, given the rarity and small number of sources in this class. Future spectropolarimetric observations of other AMP outbursts are expected to eventually detect larger phase-resolved variability. This will allow not only for accurate geometry constraints but also for testing against more complex models of local emission mechanisms. Current local models of spectropolarimetric characteristics of hot spots in AMPs (including those described in this work) are far from ideal and will require refinement with each new observation. Future work should aim to account for the temperature distribution of matter both across the spot and through its atmosphere, which affects the polarization of radiation and the shape of pulse profiles in AMPs.

After a long hiatus in soft X-ray polarimetry after sounding rockets in the 70s, *IXPE* has finally made a number of scientific discoveries in several areas of high-energy astrophysics, but AMPs remain undersampled. The satellite will continue to make observations, but it will be difficult to constrain the properties of AMPs relying only on it. The scientific community is already looking forward to the next generation of instruments. One of these will be the upcoming *Enhanced X-ray Timing and Polarimetry (eXTP)* mission (Zhang et al. 2019), which offers new advantages. Increased effective detector area will reduce the minimum detectable polarization (MDP) and allow the polarization of weaker sources to be observed. Instruments with extended energy range equipped on the *eXTP* will allow for better spectrometry of the atmospheres of neutron stars in AMPs. The wide-angle *eXTP* instruments will be able to detect transient phenomena, such as AMP outbursts, from the very beginning. This will make it possible to study the dynamics of flare evolution and changes in the polarization characteristics of the radiation in real time.

4.2 Prospects of Black Hole XRB Polarimetry

X-ray polarimetry in the field of BH-XRBs is on the verge of significant progress. Although this technique has already led to several important discoveries, it still holds enormous potential for future research.

One of the key achievements of the past two years has been the refinement of corona geometry in these systems. Observations have shown that the corona most likely has an extended structure parallel to the accretion disk, rather than elongated along the rotation axis of the BH, as previously considered in some models. However, this discovery has raised new questions about the physics and dynamics of these systems.

In particular, high degrees of polarization have been observed in several BH-XRBs. For example, in the Cygnus X-1 system, polarization of about 4% was recorded, which significantly exceeds theoretical predictions for the system's inclination. Observations of the 4U 1630−47 system showed an even greater degree of polarization of up to 10% at 8 keV (Ratheesh et al. 2024), which exceeds theoretical predictions for standard models. This has stimulated the development of new theories about the geometry and physical properties of the corona, including models with relativistic outflows and various ionization parameters. The structure, shape, and velocities of these outflows are yet to be confirmed by future observations.

Particularly impressive was the discovery related to the Cygnus X-3 system. The observation of a high degree of polarization, weakly dependent on energy, in this system led to the conclusion that it likely harbors an Ultraluminous X-ray source (ULX; Long & van Speybroeck 1983; Fabbiano 1989; Colbert et al. 2004) deep within the narrow funnel of the accretion flow (Veledina et al. 2024), see Fig. 6. The source has been observed in several spectral states from hard to ultrasoft, in which it exhibits different funnel geometries and scattering mechanisms. The flaring state remains unobserved, and observations of intermediate states, in which energy-dependent polarization might be present, are of interest. Additionally, a comprehensive explanation for the orbital variability of X-ray polarization in this system is yet to be developed. It is likely related to the rotation of the accretion funnel or to static scattering structures in a rotating frame of reference, such as the bow shock (Antokhin et al. 2022).

Figure 6. Cygnus X-3 accretion flow is being observed by *IXPE*. Image by Alexander Mushtukov.

Parallel to observations, new tools for numerical simulations of accretion flows are being developed (Liska et al. 2021; Stone et al. 2020). So are the new theoretical models for accretion structure. Polarimetry can play a key role in their verification. Many modern models provide specific predictions about changes in polarization during source state transitions, the emergence of radio jets, and other dynamic processes (El Mellah et al. 2023; Ripperda et al. 2020). For example, the magnetic reconnection in the corona may cause sharp changes in the degree and angle of polarization during flares.

It is important to note that each BH-XRB system is unique, and polarization measurements only emphasize this diversity. When we hope that data will help explain the physical processes in these systems as a whole, it is often found that some objects act as outliers, not fitting into the general picture. The new transient Swift J1727.8−1613, observed also in X-ray polarization (Veledina et al. 2023), showed an unusual behavior in soft lag evolution (Ingram et al. 2024) and the most extended continuous jet (Wood et al. 2024) for an XRB. This underscores the need for an individual approach to each system and the importance of accumulating a statistically significant sample of observations, especially in X-ray polarization. Future missions and instruments specifically designed for polarimetric observations promise to significantly enrich our understanding of the processes occurring in the immediate vicinity of BH event horizons.

5 Summary of the original publications

I Oblate Schwarzschild approximation for polarized radiation from rapidly rotating neutron stars

In this work, we described a complete and comprehensive model for calculating the observed Stokes parameters of X-ray radiation emitted from the surface of an oblate due to its fast rotation millisecond pulsar using the oblate Schwarzschild approximation (Morsink et al. 2007). We derived analytical step-by-step expressions for the PA arising from the non-spherical shape of the NS surface additionally to the polarization plane rotation due to the effects of special and general relativity. We verified our results by comparing them to full numerical general relativistic ray-tracing calculations and confirmed the significance of the oblateness for polarization pulse profile modeling. We demonstrated the biases in constraints on NS parameters such as the observer inclination and spot co-latitude, that are introduced by assuming an incorrect (spherical) shape for the star. We showed that the oblate approximation captures most of the relevant physics for polarization calculations while staying computationally efficient. Therefore, this work will be relevant for the emerging field of X-ray polarimetry of AMPs for the foreseeable future.

II Neutron star parameter constraints for accretion-powered millisecond pulsars from the simulated *IXPE* data

In this work, we applied pulse profile modeling using the Oblate Schwarzschild approximation from paper I to the simulated X-ray polarization data that can be obtained with *IXPE* from SAX J1808.4−3658. For the emission model, we used Thomson scattering in a slab geometry, including a correction for the energy shift for each scattering. We estimated the necessary exposure times for SAX J1808.4−3658 in order to obtain different accuracy in the measured Stokes parameters and inferred the constraints on the geometry of the NS. For the simulated data with 500 ks exposure, the geometrical parameters such as the inclination of the observer and the co-latitude of the spot could be determined with accuracy better than 10°. We also showed that the position of a secondary hotspot can be constrained, if it is not necessarily antipodal to the primary spot. This can also be used to further constrain the NS mass and radius and thus the EoS.

III Polarized radiation from an accretion shock in accreting millisecond pulsars using exact Compton scattering formalism.

In this study, we implement a new model for the emission of polarized radiation from AMPs. The model is based on exact solutions for radiative transport in a Comptonizing slab atmosphere for the accretion shock above the NS surface. We compute the Stokes parameters of the emergent radiation as a function of the zenith angle and energy for different values of the electron temperature, the Thomson optical depth of the slab, and the temperature of the seed blackbody photons injected at the bottom of the shock. We interpolate between a large grid computed of shock models and use the interpolated emission model in pulse profile modeling. The latter is implemented using the relativistic rotating vector model and the Oblate Schwarzschild approximation developed in paper I. As a conclusion, we estimate the constraints on the geometry of the NS from the *IXPE* data that can be obtained using the developed model. The model will be useful for the analysis of the data from future AMP-focused X-ray polarimetry missions, such as the *eXTP* mission.

IV Analytical techniques for polarimetric imaging of accretion flows in the Schwarzschild metric

In this paper, we describe an exact analytical method for calculating the observed spectropolarimetric properties of radiation from an accretion disk surface around a non-rotating BH (or a slowly rotating NS). This method is relevant for polarization imaging of BHs, such as those of M87* and Sgr A* performed by Event Horizon Telescope, and for spectra-polarimetric fitting of XRBs with weakly spinning BHs, enabled by *IXPE*. We also implement the approximate and yet highly accurate light-bending formula from Poutanen (2020) in the calculation of the observed PD and PA, making the method fully analytical. This technique can be used for spectropolarimetric fitting of XRBs due to its efficient analytical nature and high level of accuracy in Schwarzcshild metric.

V ARTPOL: Analytical ray-tracing method for spectro-polarimetric properties of accretion disks around Kerr black holes

In this manuscript, we present ARTPOL, a fast analytical ray-tracing technique for calculating the observed spectra-polarimetric properties of accretion flows around spinning (Kerr) BHs. The method extends previous work on analytical approximations for the Schwarzschild metric to include effects of BH spin, but to keep the method fully analytical and quick, avoiding time-consuming numerical integration of geodesics. We show that this technique is applicable to any optically thick accretion flow geometry for spin parameters up to $a = 0.94$. We validated this method against full numerical ray-tracing calculations and showed that it is accurate to within a few percent for a wide range of spins and inclinations. We also provide detailed comparisons for disk images, spectra, PD and PA for different spins and inclinations and study the effects of spin on polarization introduced by different parts of the accretion flow. At the same time, we tested the efficiency of our method and demonstrated that in certain cases ARTPOL can win orders of magnitude in the required computational time compared to numerical methods. Besides computational time, the analytical method provides benefits in flexibility by eliminating the reliance on precomputed tabular models. This is especially useful for fitting against multiple diverse accretion flow models, that is required in the novel field of X-ray polarimetry of XRBs, which has challenged most simple models of accretion geometry in recent years. Thus, this work provides a relevant and powerful new tool for constraining BH spins and accretion geometries using data from X-ray polarimetry missions like *IXPE*.

The author's contribution to the publications

Paper I: The author contributed to the research design of the paper and performed most of the theoretical work, implementation of the method, and writing of the manuscript. The author's contribution covers approximately 60% of the total amount of work. The article was used in the doctoral thesis of T. Salmi.

Paper II: The author contributed to the research design of the paper and performed part of the practical work related to the emission model. The author's contribution covers approximately 20% of the total amount of work. The article was also used in the doctoral thesis of T. Salmi.

Paper III: The author contributed to the research design of the paper and performed the theoretical work related to the emission model and the practical work of its implementation. The author is also responsible for writing 10% of the of the manuscript. The author's contribution covers approximately 40% of the total amount of work. The article will be used in the doctoral thesis of A. Bobrikova.

Paper IV: The author performed most of the theoretical work and practical work. The author is also responsible for writing most of the manuscript.

Paper V: The author contributed to the research design of the paper and performed most of the theoretical and practical work and wrote most of the manuscript.

List of References

Abbott, R., Abbott, T. D., Abraham, S., et al. 2020, ApJ, 896, L44
AlGendy, M. & Morsink, S. M. 2014, ApJ, 791, 78
Antokhin, I. I., Cherepashchuk, A. M., Antokhina, E. A., & Tatarnikov, A. M. 2022, ApJ, 926, 123
Baldini, L., Barbanera, M., Bellazzini, R., et al. 2021, Astroparticle Physics, 133, 102628
Bambi, C. 2018, Annalen der Physik, 530, 1700430
Barkla, C. G. 1904, Nature, 69, 463
Belloni, T. M. 2010, in Lecture Notes in Physics, Vol. 794, The Jet Paradigm - From Microquasars to Quasars, ed. T. Belloni (Berlin: Springer Verlag), 53
Beloborodov, A. M. 2002, ApJ, 566, L85
Bentz, M. C. & Manne-Nicholas, E. 2018, ApJ, 864, 146
Berdyugin, A., Piirola, V., & Poutanen, J. 2019, in ASSL, Vol. 460, Astronomical Polarisation from the Infrared to Gamma Rays, ed. R. Mignani, A. Shearer, A. Słowikowska, & S. Zane, 33
Bhattacharya, D. & van den Heuvel, E. P. J. 1991, Phys. Rep., 203, 1
Blandford, R., Meier, D., & Readhead, A. 2019, ARA&A, 57, 467
Blandford, R. D. & Payne, D. G. 1982, MNRAS, 199, 883
Blandford, R. D. & Znajek, R. L. 1977, MNRAS, 179, 433
Bobrikova, A., Loktev, V., Salmi, T., & Poutanen, J. 2023, A&A, 678, A99
Bult, P., Jaisawal, G. K., Güver, T., et al. 2019, ApJ, 885, L1
Capitanio, F., Gnarini, A., Fabiani, S., et al. 2023, Astronomy Reports, 67, S151
Chandrasekhar, S. 1931, ApJ, 74, 81
Chandrasekhar, S. 1960, Radiative transfer (New York: Dover)
Chattopadhyay, T., Kumar, A., Rao, A. R., et al. 2024, ApJ, 960, L2
Clark, J. S., Goodwin, S. P., Crowther, P. A., et al. 2002, A&A, 392, 909
Colbert, E. J. M., Heckman, T. M., Ptak, A. F., Strickland, D. K., & Weaver, K. A. 2004, ApJ, 602, 231
Costa, E. 2024, in Handbook of X-ray and Gamma-ray Astrophysics, ed. C. Bambi & A. Santangelo (Singapore: Springer), 1–20
De Rosa, R. J., Patience, J., Wilson, P. A., et al. 2014, MNRAS, 437, 1216
Dexter, J. & Agol, E. 2009, ApJ, 696, 1616
Dolence, J. C., Gammie, C. F., Mościbrodzka, M., & Leung, P. K. 2009, ApJS, 184, 387
Done, C., Gierliński, M., & Kubota, A. 2007, A&A Rev., 15, 1
Doroshenko, V., Poutanen, J., Heyl, J., et al. 2023, A&A, 677, A57
Doroshenko, V., Poutanen, J., Tsygankov, S. S., et al. 2022a, Nature Astronomy, 6, 1433
Doroshenko, V., Suleimanov, V., Pühlhofer, G., & Santangelo, A. 2022b, Nature Astronomy, 6, 1444
El Mellah, I., Cerutti, B., & Crinquand, B. 2023, A&A, 677, A67
Esin, A. A., McClintock, J. E., & Narayan, R. 1997, ApJ, 489, 865
Event Horizon Telescope Collaboration, Akiyama, K., Algaba, J. C., et al. 2021, ApJ, 910, L13
Fabbiano, G. 1989, ARA&A, 27, 87
Feigelson, E. D., Schreier, E. J., Delvaille, J. P., et al. 1981, ApJ, 251, 31
Fender, R. P., Belloni, T. M., & Gallo, E. 2004, MNRAS, 355, 1105
Fonseca, E., Cromartie, H. T., Pennucci, T. T., et al. 2021, ApJ, 915, L12
Freire, P. C. C., Ransom, S. M., Bégin, S., et al. 2008, ApJ, 675, 670
Friedman, J. L., Ipser, J. R., & Parker, L. 1986, ApJ, 304, 115

Gallo, E., Fender, R. P., & Pooley, G. G. 2003, MNRAS, 344, 60
Galloway, D. K. & Keek, L. 2021, in ASSL, Vol. 461, Timing Neutron Stars: Pulsations, Oscillations and Explosions, ed. T. M. Belloni, M. Méndez, & C. Zhang, 209–262
Giacconi, R., Gursky, H., Paolini, F. R., & Rossi, B. B. 1962, Phys. Rev. Lett., 9, 439
Gilfanov, M. 2004, MNRAS, 349, 146
Gnarini, A., Ursini, F., Matt, G., et al. 2022, MNRAS, 514, 2561
Goulding, A. D., Pardo, K., Greene, J. E., et al. 2019, ApJ, 879, L21
Gowen, R. A., Cooke, B. A., Griffiths, R. E., & Ricketts, M. J. 1977, MNRAS, 179, 303
Greene, J. E., Strader, J., & Ho, L. C. 2020, ARA&A, 58, 257
Grellmann, R., Ratzka, T., Köhler, R., Preibisch, T., & Mucciarelli, P. 2015, A&A, 578, A84
Griffiths, R. E., Ricketts, M. J., & Cooke, B. A. 1976, MNRAS, 177, 429
Hartle, J. B. & Thorne, K. S. 1968, ApJ, 153, 807
Haskell, B. & Melatos, A. 2015, International Journal of Modern Physics D, 24, 1530008
Heine, S. N. T., Marshall, H. L., Schneider, B., et al. 2024, arXiv e-prints, arXiv:2408.11168
Heinz, S., Schulz, N. S., Brandt, W. N., & Galloway, D. K. 2007, ApJ, 663, L93
Ingram, A., Bollemeijer, N., Veledina, A., et al. 2024, ApJ, 968, 76
Ingram, A. & Done, C. 2011, MNRAS, 415, 2323
Ingram, A., Done, C., & Fragile, P. C. 2009, MNRAS, 397, L101
Ingram, A. R. & Motta, S. E. 2019, NewAR, 85, 101524
Johannsen, T. & Psaltis, D. 2011, Phys. Rev. D, 83, 124015
Jourdain, E., Roques, J. P., Chauvin, M., & Clark, D. J. 2012, ApJ, 761, 27
Kaaret, P., Novick, R., Martin, C., et al. 1990, Optical Engineering, 29, 773
Kallman, T. 2004, Advances in Space Research, 34, 2673
Kalogera, V. & Baym, G. 1996, ApJ, 470, L61
Kato, S., Fukue, J., & Mineshige, S. 2008, Black-Hole Accretion Disks — Towards a New Paradigm (Kyoto: Kyoto Univ. Press)
Kerr, R. P. 1963, Phys. Rev. Lett., 11, 237
Kim, D. E., Di Marco, A., Soffitta, P., et al. 2024, Journal of Instrumentation, 19, C02028
Kormendy, J. & Ho, L. C. 2013, ARA&A, 51, 511
Kravtsov, V., Berdyugin, A. V., Kosenkov, I. A., et al. 2022, MNRAS, 514, 2479
Krawczynski, H. 2012, ApJ, 754, 133
Krawczynski, H. & Beheshtipour, B. 2022, ApJ, 934, 4
Krawczynski, H., Garson, A., Guo, Q., et al. 2011, Astroparticle Physics, 34, 550
Krawczynski, H., Muleri, F., Dovčiak, M., et al. 2022, Science, 378, 650
Lada, C. J. 2006, ApJ, 640, L63
Lattimer, J. M. & Prakash, M. 2004, Science, 304, 536
Laurent, P., Rodriguez, J., Wilms, J., et al. 2011, Science, 332, 438
Le Roux, E. 1961, Annales d'Astrophysique, 24, 71
Legg, M. P. C. & Westfold, K. C. 1968, ApJ, 154, 499
Li, L.-X., Narayan, R., & McClintock, J. E. 2009, ApJ, 691, 847
Liska, M., Hesp, C., Tchekhovskoy, A., et al. 2021, MNRAS, 507, 983
Long, K. S., Chanan, G. A., & Novick, R. 1980, ApJ, 238, 710
Long, K. S. & van Speybroeck, L. P. 1983, in Accretion-Driven Stellar X-ray Sources, ed. W. H. G. Lewin & E. P. J. van den Heuvel, 117–146
Longair, M. S. 2011, High Energy Astrophysics (Cambridge, UK: Cambridge University Press)
Lutovinov, A. A., Revnivtsev, M. G., Tsygankov, S. S., & Krivonos, R. A. 2013, MNRAS, 431, 327
Markoff, S., Nowak, M. A., & Wilms, J. 2005, ApJ, 635, 1203
Marshall, H. L., Schwartz, D. A., Lovell, J. E. J., et al. 2005, ApJS, 156, 13
Mastroserio, G., Ingram, A., & van der Klis, M. 2018, MNRAS, 475, 4027
Merloni, A., Heinz, S., & di Matteo, T. 2003, MNRAS, 345, 1057
Meszaros, P., Novick, R., Szentgyorgyi, A., Chanan, G. A., & Weisskopf, M. C. 1988, ApJ, 324, 1056
Miller, M. C. & Colbert, E. J. M. 2004, International Journal of Modern Physics D, 13, 1

Miller, M. C., Lamb, F. K., & Cook, G. B. 1998, ApJ, 509, 793
Miller, M. C. & Miller, J. M. 2015, Phys. Rep., 548, 1
Miniutti, G. & Fabian, A. C. 2004, MNRAS, 349, 1435
Mirabel, I. F. & Rodríguez, L. F. 1999, ARA&A, 37, 409
Misner, C. W., Thorne, K. S., & Wheeler, J. A. 1973, Gravitation (San Francisco: W.H. Freeman and Company)
Mitchell, D., Rochwarger, I., Sackson, M., Bischoff, G., & Bodine, O. 1976, IEEE Transactions on Nuclear Science, 23, 480
Moravec, E., Svoboda, J., Borkar, A., et al. 2022, A&A, 662, A28
Morsink, S. M., Leahy, D. A., Cadeau, C., & Braga, J. 2007, ApJ, 663, 1244
Mushtukov, A. & Tsygankov, S. 2024, in Handbook of X-ray and Gamma-ray Astrophysics, ed. C. Bambi & A. Santangelo (Singapore: Springer), 4105–4176
Mushtukov, A. A., Tsygankov, S. S., Poutanen, J., et al. 2023, MNRAS, 524, 2004
Mushtukov, A. A., Verhagen, P. A., Tsygankov, S. S., et al. 2018, MNRAS, 474, 5425
Nagirner, D. I. & Poutanen, J. 1994, Astrophysics and Space Physics Reviews, 9, 1
Narayan, R., Igumenshchev, I. V., & Abramowicz, M. A. 2003, PASJ, 55, L69
Nättilä, J. 2024, Nature Communications, 15, 7026
Nättilä, J., Steiner, A. W., Kajava, J. J. E., Suleimanov, V. F., & Poutanen, J. 2016, A&A, 591, A25
Novick, R. 1975, Space Sci. Rev., 18, 389
Novick, R., Ange, J. R. P., & Wolff, R. S. 1971, in IAU Symposium, Vol. 46, The Crab Nebula, ed. R. D. Davies & F. Graham-Smith, 54
Novick, R., Weisskopf, M. C., Berthelsdorf, R., Linke, R., & Wolff, R. S. 1972, ApJ, 174, L1
Novick, R. & Wolff, R. S. 1971, in IAU Symposium, Vol. 41, New techniques in Space Astronomy, ed. F. Labuhn & R. Lust, 159
Novikov, I. D. & Thorne, K. S. 1973, in Black Holes (Les Astres Occlus) (New York: Gordon & Breach), 343–450
Oppenheimer, J. R. & Volkoff, G. M. 1939, Physical Review, 55, 374
Özel, F. & Freire, P. 2016, ARA&A, 54, 401
Pihajoki, P., Mannerkoski, M., Nättilä, J., & Johansson, P. H. 2018, ApJ, 863, 8
Poutanen, J. 2020, A&A, 641, A166
Poutanen, J., Tsygankov, S. S., & Forsblom, S. V. 2024, Galaxies, 12, 46
Poutanen, J., Veledina, A., Berdyugin, A. V., et al. 2022, Science, 375, 874
Poutanen, J. & Vurm, I. 2009, ApJ, 690, L97
Preibisch, T., Weigelt, G., & Zinnecker, H. 2001, in IAU Symposium, Vol. 200, The Formation of Binary Stars, ed. H. Zinnecker & R. Mathieu, 69
Raaijmakers, G., Greif, S. K., Hebeler, K., et al. 2021, ApJ, 918, L29
Radhakrishnan, V. & Cooke, D. J. 1969, Astrophys. Lett., 3, 225
Ratheesh, A., Dovčiak, M., Krawczynski, H., et al. 2024, ApJ, 964, 77
Reig, P. 2011, Ap&SS, 332, 1
Ren, H. X., Cerruti, M., & Sahakyan, N. 2023, A&A, 672, A86
Reynolds, C. S. 2021, ARA&A, 59, 117
Ripperda, B., Bacchini, F., & Philippov, A. A. 2020, ApJ, 900, 100
Romanova, M. M., Ustyugova, G. V., Koldoba, A. V., & Lovelace, R. V. E. 2004, ApJ, 610, 920
Schnittman, J. D. & Krolik, J. H. 2013, ApJ, 777, 11
Schwarzschild, K. 1916, in Sitzungsberichte der Königlich Preussischen Akademie der Wissenschaften zu Berlin, 424–434
Shakura, N. I. & Sunyaev, R. A. 1973, A&A, 500, 33
Smith, J. F. & Courtier, G. M. 1976, Proceedings of the Royal Society of London Series A, 350, 421
Stone, J. M., Tomida, K., White, C. J., & Felker, K. G. 2020, ApJS, 249, 4
Sunyaev, R., Arefiev, V., Babyshkin, V., et al. 2021, A&A, 656, A132
Syunyaev, R. A. & Shakura, N. I. 1986, Soviet Astronomy Letters, 12, 117
Tananbaum, H., Gursky, H., Kellogg, E., Giacconi, R., & Jones, C. 1972, ApJ, 177, L5

Timmes, F. X., Woosley, S. E., & Weaver, T. A. 1996, ApJ, 457, 834
Tolman, R. C. 1939, Physical Review, 55, 364
Tomaru, R., Done, C., & Odaka, H. 2024, MNRAS, 527, 7047
Tsygankov, S. S., Doroshenko, V., Poutanen, J., et al. 2022, ApJ, 941, L14
Veledina, A., Muleri, F., Dovčiak, M., et al. 2023, ApJ, 958, L16
Veledina, A., Muleri, F., Poutanen, J., et al. 2024, Nature Astronomy, 8, 1031
Volonteri, M. 2010, A&A Rev., 18, 279
Walter, R., Lutovinov, A. A., Bozzo, E., & Tsygankov, S. S. 2015, A&A Rev., 23, 2
Watts, A. L. 2012, ARA&A, 50, 609
Weisskopf, M. 2018, Galaxies, 6, 33
Weisskopf, M. C., Silver, E. H., Kestenbaum, H. L., Long, K. S., & Novick, R. 1978, ApJ, 220, L117
Weisskopf, M. C., Soffitta, P., Baldini, L., et al. 2022, J. Astron. Telesc. Instrum. Syst., 8, 026002
White, T. R., Lightman, A. P., & Zdziarski, A. A. 1988, ApJ, 331, 939
Wood, C. M., Miller-Jones, J. C. A., Bahramian, A., et al. 2024, ApJ, 971, L9
Yagi, K. & Yunes, N. 2013, Phys. Rev. D, 88, 023009
Yuan, F. & Narayan, R. 2014, ARA&A, 52, 529
Zhang, S., Santangelo, A., Feroci, M., et al. 2019, Science China Physics, Mechanics, and Astronomy, 62, 29502
Zhou, S., Gügercinoğlu, E., Yuan, J., Ge, M., & Yu, C. 2022, Universe, 8, 641

TURUN
YLIOPISTO
UNIVERSITY
OF TURKU

Painosalama, Turku, Finland 2025

ISBN 978-952-02-0118-0 (PRINT)
ISBN 978-952-02-0119-7 (PDF)
ISSN 0082-7002 (PRINT)
ISSN 2343-3175 (ONLINE)